HHS Public Access

Author manuscript

J Mol Cell Cardiol. Author manuscript; available in PMC 2021 December 01.

Published in final edited form as:

J Mol Cell Cardiol. 2020 December ; 149: 95–114. doi:10.1016/j.yjmcc.2020.09.011.

Autotaxin Inhibition Reduces Cardiac Inflammation and Mitigates Adverse Cardiac Remodeling After Myocardial Infarction

Himi Tripathi[1], **Ahmed Al-Darraji**[1], **Mohamed Abo-Aly**[1], **Hsuan Peng**[1], **Elica Shokri**[1], **Lakshman Chelvarajan**[1], **Renee Donahue**[1], **Bryana M. Levitan**[1], **Erhe Gao**[2], **Gabriela Hernandez**[1], **Andrew J. Morris**[1], **Susan S. Smyth**[1], **Ahmed Abdel-Latif**[1,*]

[1]Gill Heart Institute and Division of Cardiovascular Medicine, University of Kentucky and the Lexington VA Medical Center, Lexington, KY, USA

[2]The Center for Translational Medicine, Lewis Katz School of Medicine, Temple University, Philadelphia, PA, USA

Abstract

Objective: Acute myocardial infarction (AMI) initiates pathological inflammation which aggravates tissue damage and causes heart failure. Lysophosphatidic acid (LPA), produced by autotaxin (ATX), promotes inflammation and the development of atherosclerosis. The role of ATX/LPA signaling nexus in cardiac inflammation and resulting adverse cardiac remodeling is poorly understood.

Approach and Results: We assessed autotaxin activity and LPA levels in relation to cardiac and systemic inflammation in AMI patients and C57BL/6 (WT) mice. Human and murine peripheral blood and cardiac tissue samples showed elevated levels of ATX activity, LPA, and inflammatory cells following AMI and there was strong correlation between LPA levels and circulating inflammatory cells. In a gain of function model, lipid phosphate phosphatase-3 (LPP3) specific inducible knock out (Mx1-Plpp3^{Δ}) showed higher systemic and cardiac inflammation after AMI compared to littermate controls (Mx1-Plpp$3^{fl/fl}$); and a corresponding increase in bone marrow progenitor cell count and proliferation. Moreover, in Mx1- Plpp3^{Δ} mice, cardiac functional recovery was reduced with corresponding increases in adverse cardiac remodeling and scar size (as assessed by echocardiography and Masson's Trichrome staining). To examine the effect of ATX/LPA nexus inhibition, we treated WT mice with the specific pharmacological inhibitor, PF8380, twice a day for 7 days post AMI. Inhibition of the ATX/LPA signaling nexus

[*]**Corresponding author at:** Associate Professor of Medicine, Division of Cardiology, University of Kentucky and the Lexington VAMC, 741 S. Limestone Street, BBSRB, Room 349, Lexington, KY 40536-0509, abdel-latif@uky.edu.

Disclosures:
None.

Supplementary data
Supplementary material

resulted in significant reduction in post-AMI inflammatory response, leading to favorable cardiac functional recovery, reduced scar size and enhanced angiogenesis.

Conclusion: ATX/LPA signaling nexus plays an important role in modulating inflammation after AMI and targeting this mechanism represents a novel therapeutic target for patients presenting with acute myocardial injury.

Graphical abstract:

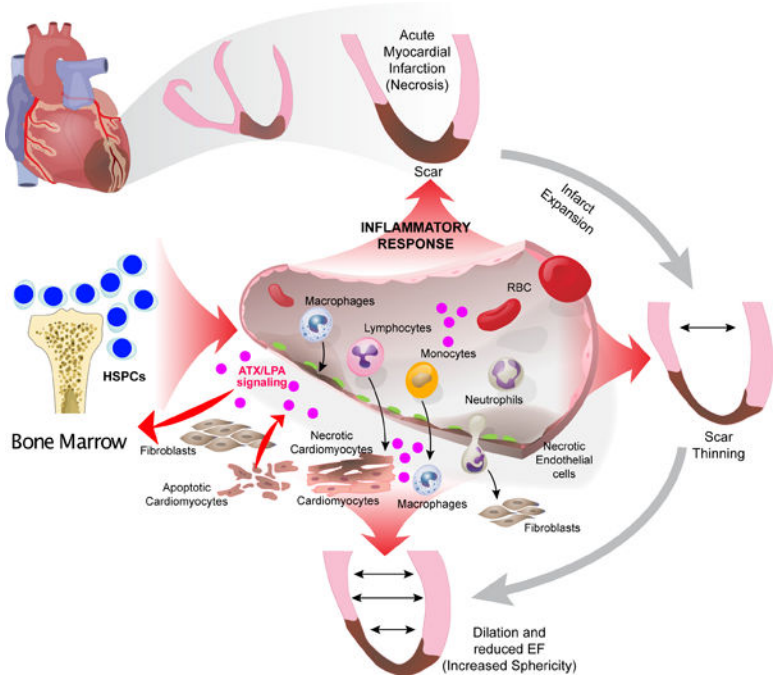

Schematic summarizing the role of autotaxin/lysophosphatidic acid signaling in post-AMI inflammation and cardiac dysfunction. Damage associated molecular pattern molecules released from dying cardiomyocytes and cardiac fibroblasts initiate an inflammatory cascade resulting in the activation of Autotaxin/Lysophosphatidic acid signaling; which in turn augments local and systemic inflammation through the release of inflammatory cytokines and chemokines. Systemically, activation of bone marrow progenitors results in increased production of inflammatory cells. Locally, increased chemoattractants such as MCP-1 results in increased infiltration of inflammatory cells to the damaged myocardium. Collectively, these events result in prolonged and exacerbated inflammatory response and impaired cardiac functional recovery.

Keywords

autotaxin; lysophosphatidic acid; myocardial infarction; inflammation; heart failure

1. INTRODUCTION

Acute myocardial infarction (AMI) which commonly leads to heart failure (HF), is among the leading causes of morbidity and mortality worldwide. While the innate immune response after AMI is essential for clearing necrotic cells and initiating myocardial repair, uninhibited

inflammatory response is often complicated by adverse ventricular remodeling and HF. The initial sterile inflammatory reaction to AMI involves toll-like receptor signaling, complement activation and generation of reactive oxygen species which result in upregulation of cytokines and chemokines leading to additional cell necrosis. Post-AMI inflammation is a well-orchestrated response consisting of 3 distinct waves of immune cells infiltrating the myocardium: neutrophils peaking at day 1 followed by pro-inflammatory monocytes ($Ly6C^{high}$) which turn into pro-inflammatory tissue macrophages peaking at day 3 and eventually anti-inflammatory monocytes/macrophages ($Ly6C^{lo}$) peaking at day 7 after injury [1, 2]. Despite significant advances in the management of patients with AMI, therapies aimed at modulating the detrimental prolonged inflammatory response are lacking.

Autotaxin (ATX), encoded by the ectonucleotide pyrophosphatase/phosphodiesterase 2 (ENPP2) gene, has lysophospholipase D activity which hydrolyzes lysophosphatidylcholine (LPC) to generate the bioactive lipid mediator lysophosphatidic acid (LPA) [3]; and is a major source of extracellular LPA. LPA activity is mediated by G protein-coupled receptors (LPA1–6 receptors). The ATX/LPA signaling nexus plays an important role in the development of cardiovascular diseases [4]. Specifically, LPA plays an important role in mediating cardiac dysfunction and hypertrophy by suppressing autophagy through activation of the LPA receptor 3 (LPA_3) and AKT/mTOR pathways [5]. Additionally, genetic deficiency of LPP3, an enzyme that can inactivate LPA, in endothelial and smooth muscle cells resulted in compromised vascular barrier function and increased the number of leukocytes and pro-inflammatory cytokines/chemokines in the vessel wall [6, 7], leading to increased plaque size and development of atherosclerosis [8, 9]. Moreover, the plasma LPA concentration was found to be elevated in AMI patients, peaking 48–72 hours post AMI, albeit the significance of this phenomena is not fully understood [10]. These findings suggest that ATX/LPA signaling may play a role in the inflammatory cascade following AMI. Targeting this mechanism with existing receptor antagonists and enzyme inhibitors might be therapeutically feasible to circumvent the development of heart failure.

In this study, we provide the first evidence that the ATX/LPA signaling nexus plays an important role in modulating inflammation following myocardial ischemic injury; resulting in adverse cardiac remodeling and the development of heart failure. Our studies using specific pharmacological inhibition of ATX/LPA signaling resulted in inflammation resolution and attenuation of cardiac adverse remodeling post-MI. These findings represent an important step in the development of clinically relevant therapies to modulate the prolonged inflammatory response after myocardial ischemic injury and the resulting heart failure.

2. MATERIALS AND METHODS

Full details on the materials and methods are included in supplemental materials.

2.1 Animals

8–10-week female C57BL/6 mice (Jackson Laboratory, Bar Harbor, ME) were used in the study. To generate a Plpp3 null allele in adult animals, $Plpp3^{fl/fl}$ mice were crossed with transgenic mice expressing Cre recombinase under the control of Mx1 promotor (Mx1-Cre,

strain # 003556) to generate Mx1- Plpp3$^{\Delta}$ mice [7, 11]. All newborn mice were treated with 10mg/mL polyinosinic-polycytidylic acid (pI:pC) (Sigma, P1530) and 50 μL was administered via intraperitoneal (i.p.) injection on post-natal days 3 to 5. Control mice are MX1- $^{fl/fl}$ who do not have deletion of LPP3 served as controls for all comparisons with Mx1- Plpp3Δ that have LPP3 gene deletion. This was done to negate the effect of cre and polyinosinic-polycytidylic acid (pI:pC) injection in our studies. The literature confirms that LPP3 tissue expression and level does not differ between male and female mice and that LPP3 deletion using the Mx1-cre model occurs evenly in both sexes [12]. Indeed, studies showed no difference in the phenotype, inflammatory or atherosclerotic response of LPP3 KO male and female mice [13]. Hence, we focused our studies on female mice due to their superior survival rates and to reduce the overall animal numbers as requested by our institutional IACUC. All experiments were approved by the University of Kentucky IACUC.

2.2 Human studies

The study population consists of 40 patients with acute ST-elevation myocardial infarction (STEMI) enrolled at the University of Kentucky hospitals between January 2014 and July 2015. Samples were collected at the time of presentation to the hospital (0 hours; within 6 hours from onset of symptoms) then at 3, 6, 12, 24 and 48 hours after presentation. Five matched controls with similar comorbidities but no active myocardial ischemia/infarction were included in the analysis. The study protocol complies with the Declaration of Helsinki and was approved by the University of Kentucky's Institutional Review Board and Ethics Committees. All patients provided written informed consent.

2.3 Murine model of myocardial infarction

Mice underwent permanent left anterior descending artery (LAD) ligation as previously described [14]. Mice were anesthetized with 1–3% isoflurane using a small animal vaporizer system. Pain reflexes were examined to make sure that the mouse is adequately anaesthetized prior to surgery. Animals were treated with pain medicine for 48 hours after surgery. This duration was prolonged if animals showed signs of pain, discomfort or reduced food or water intake. The sham group underwent the same surgical procedure except the suture was passed under the LAD but not tied. Postoperatively, mice were monitored for behavior changes (pain or stress).

2.4 Autotaxin Inhibitor PF 8380 treatment

Following AMI, WT mice were randomized to receive either PF8380 (Cayman Chemical, Ann Arbor, MI, USA), a potent and specific autotaxin inhibitor, at (10 mg/kg i.p. twice daily) [15] or vehicle (2% Beta-Cyclodextrin with 0.1% Tween 80 in PBS) started immediately after AMI and continued for 7 days. A subgroup of mice was injected daily with BrdU (Sigma B9285) at (80 mg/kg, i.p.) beginning the day of operation for total of 7 days. Animals were sacrificed at 30 days after the operation via CO_2 asphyxiation followed by cervical dislocation.

2.5 Histology

Mice (N = 10–12 per group) were sacrificed 30 days after AMI. Following echocardiography, hearts were harvested as previously described [16]. Hearts were stained against: Rabbit anti-mouse IBA1 (Novus Biologicals, CO) overnight at 4°C. After washing, sections were incubated with secondary antibody conjugated to Alexa Fluor 488 (1:500, Invitrogen, Carlsbad, CA), then incubated with Sudan Black B (Sigma Aldrich, St. Louis, MO) for 30 minutes and subsequently incubated with DAPI nuclear counterstain. A similar protocol was used to prepare heart sections from mice on baseline, day 7 and day 30 for capillary density assessment using FITC- Isolectin B4 (FL1201, Vector Labs, Burlingame, CA). Apoptotic cells in heart sections were identified at day 1 by terminal deoxynucleotidyl transferase-mediated dUTP nick end-labeling (TUNEL) staining using the In-Situ Cell Death Detection Kit and α-sarcomeric actin (1:200 dilution, Sigma Aldrich, St. Louis, MO) according to the manufacturer's protocol. DAPI counterstaining was followed by a final PBS wash.10–15 adjacent pre-infarct and remote zones per section were analyzed (1–2 sections/animal) at 40x magnification using Nikon Confocal Microscope A1 in the University of Kentucky Confocal Microscopy facility.

2.6 Echocardiography

Echocardiograms were performed using a Vevo 3100 system (Visual Sonics, Toronto, CA) equipped with a MX550D 25–55 MHz linear array transducer. *In vivo* cardiac function was assessed at baseline before cardiac surgery, 48 hours post-AMI and immediately prior to sacrifice 30 days post-AMI by echocardiography. Echocardiography was performed with mice under 1–3% isoflurane anesthesia. All echocardiography analyses were performed by a blinded investigator.

2.7 Measurement of LPA and Sphingosine-1 phosphate

Murine peripheral blood (PB) samples were obtained from the retro-orbital plexus into tubes containing 1:5 ratio of EDTA: CTAD. Plasma was isolated by centrifuging whole blood for 10 min at 800 x *g*. Supernatant was then removed and centrifuged at 9,400 x *g* for 10 min to remove platelets, and the supernatant was then used for lipid measurements. Lipids were extracted from plasma using acidified organic solvents and analyzed using mass spectrometry, as previously described [17].

2.8 Autotaxin activity assay

ATX activity was measured in human plasma, mouse plasma, heart and bone marrow cells and supernatant by choline release assay [18] in which choline is oxidized to betaine and hydrogen peroxide. Plasma was isolated as detailed above and murine bone marrow was harvested from the tibia and fibula by centrifugation at 5000 x g for 30 sec followed by incubation in PBS for 10–15 minutes then supernatant was collected. BM cell lysate was prepared in RIPA buffer supplemented with protease inhibitors cocktail (Sigma-Aldrich). Protein concentration was determined with a BCA protein assay kit (Thermo-Fischer Scientific) using BSA as standard. BM cell homogenate (20 μg protein in 20 μl of 10mM Tris HCl, pH 7.4) and supernatant was separated for measuring ATX activity.

2.9 Flow Cytometry.

Heart tissues collected at 1, 3 and 7 days after AMI were harvested, digested to single cell suspension and prepared for staining. Heart cells were stained against the following antibodies: CD45 APCCy7 (BioLegend, 103116), CD115 PE (BioLegend, 135506), CD11b APC (Biolegend, 101212), F4/80 PECy7 (BioLegend, 123114), Ly-6G/Ly- 6C PerCP/Cy5.5 (BioLegend, 108428), Ly6G FITC (Biolegend;, 127606), CD206 PE (Biolegend, 141706), and CD86 PerCP- CY5.5 (Biolegend, 105028). $CD45^{hi}/Ly6G^{lo}/F4\text{-}80^{hi}$ cells were identified as macrophages and further classified as activated/pro-inflammatory based on the expression of CD11b and CD86. Neutrophils were defined as $CD45^{hi}/CD115^{lo}$/Ly6-C/G^{lo}. Pro-inflammatory monocytes are defined as $CD45^{hi}/CD115^{hi}$/Ly6-C/G^{hi}.

Bone marrow cells were isolated at the above-mentioned time points and resuspended in PBS containing 2% fetal bovine serum (FBS). Cells were stained against CD117 (c-Kit) APC/Cy7 (Biolegend, 105826), Ly-6A/E PE/Cy7 (Sca-1) (Biolegend, 108114), CD34 PerCP/Cy5.5 (Biolegend, 128608), CD16/32 PE (Biolegend, 101308) and BrdU APC (e-biosciences, 17-5071-42). All anti-mouse lineage markers (Lin) were FITC conjugated and purchased from BD Pharmingen: anti-CD45R/B220 (553088); anti-T-cell receptor β (553170); anti-TCRγδ (553177); anti-CD11b (553310); anti-Ter-119 (557915); anti-Ly6C/G (553127). Given the variability in the number of cells harvested from BM, we elected to report the number of progenitors as cells/ 1 million total number of cells harvested.

For human peripheral blood inflammatory monocytes and granulocyte quantification, PB samples were stained against CD14 PE (Biolegend, 301806), CD16 FITC (Biolegend, 302006), HLA DR APC/Cy7 (Biolegend, 307618), CD 42b (Biolegend, 303916), CCR2 PerCP/Cy5.5 (Biolegend, 357204), and CD11b APC (Biolegend, 301310). Granulocytes were defined based on the forward and side scatter (FSC-SSC) plots of PB cells after lysis of red blood cells. We conducted confirmatory studies for neutrophils which were defined as CD45+/HLA-DR−/CD14−/CD15+ which 100% backgated to the granulocyte gate in the FSC-SSC plots (Suppl. Fig. 1). Monocytes were defined as CD45+/HLA-DR+ and then subdivided based on the expression of CD14 and CD16 into classical (CD14++/CD16−), intermediate (CD14+/CD16+) and non-classical (CD16++/CD14−). Granulocytes and monocyte subpopulations were then divided based on their expression of CCR2, CD11b and CD42 for leukocyte-platelet aggregates.

All samples were acquired using an LSR II (Becton Dickinson, Mountainview, CA) system and analyzed using FlowJo (version 7) software to generate dot plots and analyze the data.

2.10 Real-time PCR

Total mRNA was isolated from the PB, heart and spleen cells with PureLink RNA Mini Kit (Life technologies, USA) and reverse-transcribed with Syber Green Master Mix Reagent (Thermo Fisher Scientific, USA). Then, cDNA was synthesized using SuperScript VILO cDNA synthesis kit (Invitrogen). Quantitative assessment of mRNA expression of markers characterizing Autotaxin, interferon (α and β), proinflammatory cytokines (IL-1β, MCP-1,

TNF-α), LPP3 and control 18-S RNA was performed by qRT-PCR using a Quant Studio 7 Flex real time thermocycler (Applied Biosystems, Foster City, CA).

2.11 Cell culture

Bone marrow derived macrophages (BMDMs) were used for the *in vitro* studies. Differentiated cells were treated with LPA (5 μM) (Avanti Polar Lipids, AL) and PF8380 (10 μM) (Sigma-Aldrich, St. Louis, MO) for 6 hours at 37 C with 5 CO2 Supernatants were collected to assess the cytokines levels and their ratio (TNF-α and IL-10) using ELISA assays (BD Biosciences, San Deigo, CA) according to the manufacturer's protocol. Data are presented as cytokine ratio.

2.12 In vitro transwell cell migration assay

Chemotaxis experiments were performed using a Boyden chamber (24-well chemotaxis chamber) with 8 μm pore size polycarbonate membranes (Costar, CLS3422). Bone marrow derived macrophages (2.5×10^5 cells/ml) were seeded in100 μl of DMEM media and introduced into the upper compartment of the trans-well. Chemotaxis towards MCP-1 (20 ng/ml), MCP1 and PF 8380 (10μM), or negative control (0.1% FBS) was examined by quantifying cells using a light microscope with a 20x objective.

2.13 Western blotting

Wild type and LPP3 KO mouse heart tissues (~ 50 mg) were homogenized in RIPA buffer with protease inhibitors (pepstatin, leupeptin and aprotinin, and pefabloc® SC) and lysates were centrifuged at 15,000 rpm for 30 min. Equal amounts of tissue lysate (BCA protein estimation; BioRad; Hercules, CA) were run on 10% SDS-PAGE gels, transferred to nitrocellulose, blocked with 5% milk/TBST (0.1%), and finally incubated with antibodies at the following concentrations: LPP3 (1:500 in 5% Milk for 2 hours at room temperature), and β-Tubulin (Invitrogen) (1:5000 in 0.2% Tween overnight at room temperature). The membrane was subsequently incubated with secondary antibody conjugated to horseradish peroxidase at 1:3,000 dilution in 0.1% TBS-Tween 20 for 1 hour at room temperature. Protein bands were visualized on X-ray films using the enhanced chemiluminescence system (Thermo Scientific).

2.14 Statistical analysis

Throughout the manuscript, data are expressed as mean ± standard error of the mean (SEM). Differences were analyzed using the unpaired Student *t*-test or analysis of variance (one way or multiple comparisons repeated measures) as appropriate. Post hoc multiple comparison procedures were performed using 2-sided Dunnett or Dunn tests as appropriate with control/vehicle groups as the control category Correlation analyses were performed using the Pearson's correlation for normally distributed variables and Spearman's correlation for non-normally distributed variables. A value of $P < 0.05$ was considered significant. Statistical analyses were performed using the Prism 8 package (GraphPad, La Jolla, CA) and SPSS version 25 (SPSS, IBM Corp, Armonk, NY).

3. RESULTS

3.1 LPA, autotaxin activity, and circulating inflammatory cells are upregulated after acute myocardial infarction in humans.

LPA plays an important role in the development of atherosclerotic disease which is widely regarded as an inflammatory process [19, 20]. However, the role of LPA in mediating post-AMI inflammation has not been previously examined. To examine the ATX/LPA signaling nexus post-AMI, we enrolled 40 patients with AMI (ST elevation myocardial infarction) or matched controls (Table 1). Control subjects were generally younger but had similar incidence of comorbidities. Plasma LPA levels were higher at presentation in AMI patients and steadily declined over 48 hours to levels observed in matched controls (Fig 1A). A detailed breakdown of various measured LPA species is summarized in Suppl Fig 2. Of note, plasma LPA levels showed a trend towards higher levels in males, but this trend did not achieve statistical significance (Suppl Fig 3A). Elevated peak LPA levels correlated with plasma ATX concentration, assessed by ELISA, which were significantly higher in patients with LPA level above the median (775.2 ± 37.2 vs. 435.2 ± 25.9 ng/ml $P<0.001$; Fig 1B). Similarly, ATX activity was elevated in correlation with increase in plasma LPA (Suppl Fig 3B). This data indicates that the ATX/LPA signaling nexus is activated during AMI in humans. AMI is also associated with leukocytosis, and in particular monocytosis [21]. Therefore, we measured circulating numbers of monocytes, granulocytes and their subsets in peripheral blood of our cohort. Circulating PB inflammatory monocytes, granulocytes and monocyte-platelet aggregates peaked within the first 24 hours following revascularization for AMI in humans (Fig 1C). Furthermore, we observed strong correlation between plasma LPA levels at presentation and different subsets of PB inflammatory cells after AMI (Table 2). Collectively, these observations are consistent with the activation of the ATX/LPA nexus after AMI. To dissect the role of ATX/LPA signaling in post-AMI inflammatory response, we conducted mechanistic studies in a preclinical murine model of myocardial injury.

3.2 AMI initiates a signaling cascade resulting in the activation of ATX/LPA nexus.

Plasma LPA levels show dynamic increase in humans after AMI [10]; however, the mechanisms of this elevation are poorly understood. Earlier studies have shown that the infarcted heart produces damage-associated molecular patterns (DAMPs), activating the complement cascade and toll-like receptors (TLRs), resulting in an intense inflammatory reaction [22]. In response to toll-like receptor activation, ATX is transcribed in immune cells, through a type I interferons (IFNs) autocrine-paracrine loop involving the JAK-STAT and PI3K-Akt pathways [23]. In our studies, AMI was associated with higher expression of IFN-α (5 5±1.1-fold change, $p< 0.01$) and IFN-β (4±1.6-fold change, $p< 0.01$) in the heart 3 days after acute injury (Fig. 2A). Interestingly, the increased expression of IFNs was associated with a corresponding increase in the expression of ATX in PB cells (2.6-fold increase compared to sham, $p< 0.01$) (Fig. 2B). Additionally, the activity of ATX corresponded with increased gene expression and inflammation in heart tissue after AMI, peaking at 3 days after injury (Fig 2C). These changes are in agreement with prior reports in the literature confirming the increased expression and activity of ATX in inflammatory conditions [24] and cancer [25].

3.3 Lipid phosphate phosphatase 3 deletion is associated with increased number of inflammatory cells after AMI secondary to enhanced myelopoiesis.

Lipid phosphate phosphatase 3 (LPP3), encoded by the phospholipid phosphatase 3 (Plpp3) gene, can dephosphorylate extracellular LPA and plays a major role in the tight regulation of its levels [7]. To explore the role of LPA signaling after AMI, we performed LAD ligation on 6–8-week-old Mx1-Plpp3$^{\Delta}$ and Mx1-Plpp3$^{fl/fl}$ mice. MX-1-mediated inactivation of Plpp3 was confirmed by PCR analysis (Fig 3A) and western blotting (Fig 3B). First, we examined LPP3 expression in heart and PB cells in these mice post-AMI and observed an increase in LPP3 expression with AMI. However, the LPP3 response was blunted in Mx1-Plpp3$^{\Delta}$ compared to Mx1-Plpp3$^{fl/fl}$ (Fig 3C). The balance between pro-inflammatory (Ly6C^{hi}) and anti-inflammatory (Ly6C^{lo}) monocyte subpopulations is key to cardiac recovery after AMI [1]. We analyzed the number of inflammatory cells in cardiac tissue at 1, 3 and 7 days following induction of AMI using flow cytometry and IHC and observed a significant increase in the number of Ly6C^{hi} monocytes (CD45^{+}/Ly6C/G^{hi}/CD115^{hi}, $p<0.001$), pro-inflammatory macrophages (CD45^{+}/F4-80^{+}/CD11b^{+} cells, $p<0.0001$ and CD45^{+}/F4-80^{+}/CD86^{+} cells, $p<0.05$) and neutrophils (CD45^{+}/CD115^{lo}/Ly6C/G^{hi}, $p<0.05$ d-1; $p<0.01$) in cardiac tissue of Mx1- Plpp3$^{\Delta}$ compared to Plpp3$^{fl/fl}$ littermate controls (Fig 3D). On the other hand, we observed significant reduction in anti-inflammatory Ly6C^{Lo} monocytes (CD45^{+}/Ly6C/G^{Lo}/CD115^{hi}, $p<0.001$) in Mx1-Plpp3$^{\Delta}$ mice. No significant difference in cardiac inflammatory cells was observed between groups at baseline. However, it is important to note that our flow cytometry analyses did not allow us to differentiate between BM-derived and resident cardiac macrophages [26]. We then conducted confirmatory IHC staining for cardiac macrophages using the pan-macrophage marker IBA1 [27] on day 3 post-AMI. In agreement with our flow cytometry data, we observed significantly higher numbers of IBA1+ macrophages in the peri-infarct region ($p<0.0001$) and remote zone ($p<0.01$) of Mx1-Plpp3$^{\Delta}$ Vs. Mx1-Plpp3$^{fl/fl}$ mice (Fig 3E and F). Macrophage polarization plays an important role in cardiac response to ischemic injury. Anti-inflammatory macrophages produce multiple cytokines and anti-apoptotic factors that reduce cell death in the peri-infarct region. We assessed the TUNEL positive cells in the peri-infarct region in Mx1-Plpp3$^{\Delta}$ and littermate controls and observed significantly higher numbers of apoptotic cells in Mx1-Plpp3$^{\Delta}$ mice ($p<0.0001$) (Fig 3G and H).

The elevated number of cardiac inflammatory cells particularly monocytes and neutrophils, led us to examine the state of their progenitors in the bone marrow. Therefore, we analyzed BM hematopoietic stem/progenitor cells (HSPCs), common myeloid progenitors (CMPs) and granulocyte macrophage progenitors (GMPs) (Fig 4A) to determine if the elevated numbers of inflammatory cells are secondary to myelopoiesis. Following AMI, we observed an increase in the number of BM derived progenitors, peaking at the first day post-AMI. This increase was more pronounced in Mx1-Plpp3$^{\Delta}$ compared to Mx1-Plpp3$^{fl/fl}$ mice (Fig 4B). To determine if the increase in number of myeloid progenitors is due to their proliferation, we injected mice with BrdU daily after AMI. BrdU incorporates into proliferating DNA in place of thymidine and therefore labels cells that divide after the BrdU pulse. Flow cytometric analysis of BrdU demonstrated higher percentage of BrdU+ HSPCs, GMPs and CMPs corresponding to the increased number of progenitors in the BM. Compared to Mx1-Plpp3$^{fl/fl}$ mice, Mx1-Plpp3$^{\Delta}$ demonstrated significantly higher percentage

of BrdU+ progenitors (Fig 4C). This data suggests that elevated LPA, through the deletion of LPP3, increases systemic inflammatory cells through stimulating proliferation of HSPCs in the BM.

3.4 LPP3 deletion is associated with impaired cardiac healing after AMI.

Multiple studies have linked exacerbated inflammation with worse cardiac functional recovery and clinical outcomes in humans and animals [28, 29]. To investigate the long-term effects of Plpp3 deletion and exacerbated post-AMI inflammation on cardiac function, we performed echocardiograph at baseline, 48 hours and 4 weeks after injury (Fig 5A). Both groups had similar cardiac function at baseline and a significant reduction in cardiac functional parameters at 48 hours post-AMI. However, the reduction in global cardiac function and adverse cardiac remodeling in Mx1- $Plpp3^{\Delta}$ mice persisted until 30 days after AMI resulting in significantly worse cardiac function compared to $Plpp3^{fl/fl}$ littermate controls. We observed reduction in LV ejection fraction (26.4±4.7% vs. 47.7±5.7%, $P<0.01$) as well as fractional shortening (10.8±2.5% vs. 19.96±3.4%, $P<0.05$). These functional changes were echoed by parameters of LV remodeling such as increased end-systolic diameters (4.8±0.4, 3.5±0.4 mm; $P<0.01$), anterior wall thickness during systole (1.1±0.1, 0.85±0.1 mm; $P<0.05$) as well as posterior wall thickness during systole (1.1±0.1, 0.79±0.1 mm; $P<0.01$, Fig 5B) in Mx1- $Plpp3^{\Delta}$ mice compared to the littermate control group. Other echocardiography parameters are summarized in Table 3. Additionally, we conducted an analysis were echocardiographic parameters were compared to baseline function in each animal. The results of this analysis are outlined in Suppl Fig 4 and show similar pattern of worse cardiac recovery in Mx1- $Plpp3^{\Delta}$ mice.

Appropriate and timely resolution of the inflammatory response following AMI is critical for myocardial angiogenesis and proper wound healing. Therefore, we assessed myocardial capillary density in the peri-infarct area using the endothelial-specific FITC-isolectin B4 antibody at day 30 post-AMI. The data revealed that the capillary density in Mx1- $Plpp3^{\Delta}$ mice was significantly lower compared to the control group (158±6.2 vs. 129±9 capillaries/mm^2, $P<0.05$, Fig 5C and D). Of note, there was no difference in capillary density in these mice at baseline (Suppl Fig 5). We further investigated the effect of exacerbated inflammation on cardiac fibrosis and healing by examining scar formation using Masson trichrome staining. At 30 days after AMI, Mx1- $Plpp3^{\Delta}$ mice had larger scar size compared to $Plpp3^{fl/fl}$ controls (17.4±2.5 vs 8.1±1.2; $P<0.05$, Fig 5E). Taken together, LPP3 deletion is associated with exacerbated inflammation, which could explain the impaired angiogenesis, adverse cardiac remodeling and larger scar observed 30 days post-AMI.

3.5 ATX inhibition results in attenuated inflammatory response after AMI.

Inhibition of ATX/LPA signaling axis has been implicated as a therapeutic target in several chronic inflammatory and fibrotic disorders. To investigate the therapeutic role of inhibiting ATX/LPA signaling after AMI, WT mice underwent permanent LAD ligation and were then randomized to receive PF8380 (10 mg/kg i.p. twice daily) or vehicle starting immediately after surgery for 7 days post-AMI (Fig 6A). Initially, we confirmed the systemic ATX inhibition by examining plasma LPA levels and ATX activity in both groups. In agreement with other reports [15, 30], LPA levels were significantly decreased with PF8380 treatment

(P<0.05) and corresponded with significant reduction in plasma ATX activity (Fig 6B, P<0.01). In addition, BM ATX activity was elevated in AMI and corresponded with early BMSPC activation and proliferation (Fig 6C). ATX inhibition blunted this activity, specifically during the first 3 days after AMI. Interestingly, we did not observe significant changes in the plasma level of the bioactive lipid, sphingosine-1 phosphate, with ATX inhibition or the deletion of LPP3 after AMI (Suppl Fig 6).

We examined the effect of ATX inhibition on cardiac infiltration of inflammatory cells using flow cytometry (Fig 7A). We observed a reduction in the number of cardiac neutrophils ($CD45^+/CD115^{lo}/Ly6G/C^{hi}$, p<0.05) and $Ly6C^{hi}$ monocytes ($CD45^+/Ly6C/G^{hi}/CD115^{hi}$, p<0.05) in the PF8380 treated mice compared to vehicle controls. Furthermore, we observed a decrease in activated macrophages ($CD45^+$/ $F4\text{-}80^+/CD11b^+$, P<0.01 on days 1 and 3; (Fig 7B) in the PF8380 treated group. This data suggests a therapeutic potential for the inhibition of the ATX/LPA signaling axis after AMI. It is important to note that the dynamics of cardiac macrophages were different from previous reports in the literature [1], which could be explained by the surgical technique and degree of injury.

3.6 ATX inhibition decreased myelopoiesis after AMI.

Pro-inflammatory cytokines play a crucial role in initiating and maintaining the post-AMI inflammatory response. Cytokines like IL-1β play an important role in inducing myeloid progenitor cell proliferation in response to tissue injury and augment the production of neutrophils and monocytes [2, 31], thus fueling the exacerbated inflammatory response [32]. Additionally, local chemokines such as macrophage chemoattraction peptide (MCP-1) in the heart are essential for the chemoattraction of inflammatory cells. Therefore, we investigated the effect of ATX inhibition on local and systemic expression of pro-inflammatory cytokines using quantitative real-time polymerase chain reaction (qPCR). Our studies demonstrated significant reduction in gene expression of IL-1β, MCP-1 and TNF-α in the heart (Fig 7C, P<0.05) and MCP-1 and TNF-α in the spleen 3 days after AMI in the PF8380 treated group (Fig 7D, P<0.01). The reduction in these chemokines can explain changes noted in cardiac inflammatory cells detailed above. Next, we conducted IHC studies on cardiac tissue 3 days after AMI to quantify macrophages and examine their spatial distribution. We observed significantly lower numbers of cardiac macrophages in the peri-infarct region with ATX inhibition (Fig 7E, p<0.05).

Given the reduced expression of IL-1β in PF8380-treated mice and the corresponding reduction in inflammatory cells, we sought to examine the number and proliferation of BM progenitors. We observed significant reduction in the absolute numbers of BM HSPCs (p<0.001), CMPs (p<0.001) and GMPs (p<0.01) with ATX Inhibition (Fig 7F and G). These changes were secondary to significant reduction in the proliferation of these populations as assessed by BrdU intracellular staining, which reflected the reduction in percentage of BrdU positive progenitors.

3.7 ATX inhibition in bone marrow derived macrophages reduced their inflammatory response and cell migration *in vitro*.

Activation of ATX enhances LPA production in the cellular microenvironment resulting in exacerbated inflammatory response [23, 24]. Using primary bone marrow-derived macrophages (BMDMs) we assessed the effect of ATX inhibition on their inflammatory response using a well-established *in vitro* model [33]. Studies have shown that macrophage response to inflammatory stimuli *in vitro* is predictive of their *in vivo* behavior [34]. Six hours after LPS + INFγ stimulation, we observed a shift in BMDMs towards the pro-inflammatory phenotype and a significant increase in the ratio of TNF-α/IL-10 production Then we examined the effect of LPA (5 μM) treatment with and without the specific ATX inhibitor, PF8380 (10 μM), on BMDMs LPA supplementation was associated with an exacerbated inflammatory response in BMDMs and a significantly higher TNF-α/IL-10 ratio. With PF8380 treatment, BMDMs demonstrated an attenuated inflammatory response (Fig 7H, $p<0.05$). NFκB signaling plays a critical role in the pro-inflammatory changes observed in macrophages which are initiated by its translocation from the cytoplasm to the nucleus [35]. Therefore, we examined the effect of ATX/LPA signaling on NFκB translocation in macrophages stimulated with various pro-inflammatory signals. Macrophages exposed to LPS or LPA demonstrated significant reduction in the cytoplasmic to nuclear NFκB ratio suggesting its translocation. Treatment with PF8380 or NFκB inhibitor blunted this translocation (Suppl Fig 7). Additionally, we investigated the effect of ATX inhibition on macrophage migration. BMDMs treated with PF8380 showed decreased cell migration towards MCP-1 gradient in Boyden migration assays (Fig 7I, $p<0.01$). These findings suggest that ATX signaling plays an important role in macrophage polarization and migration, which could explain the cellular changes observed in our *in vivo* studies. Mechanistically, these results support the pro-inflammatory role of ATX/LPA signaling and suggest a therapeutic potential for its inhibition in inflammatory conditions.

3.8 ATX inhibition improved cardiac recovery after AMI.

To investigate the long-term effects of ATX inhibition post-AMI on cardiac function, we performed echocardiography at baseline, 48 hours and 30 days after AMI (Fig 8). Both groups had similar reduction in cardiac functional parameters at 48 hours after acute injury. In comparison to vehicle-treated mice, which showed progressive deterioration in cardiac function, we observed stabilization of cardiac functional parameters in the PF8380 treated group. This benefit was evident on the global cardiac functional parameters such as the LV ejection fraction (46.6±3.3% vs. 33.8±5.5%, $p<0.05$) as well as adverse remodeling parameters such as the LV end systolic (3.5±0.2 vs. 4.4±0.4 mm, $p<0.05$), end diastolic diameters (4.4±0.1 vs. 5.3±0.3 mm, $p<0.01$; Fig 8B), anterior wall (0.91±0.1, 1.26±0.1 mm; $P<0.0001$) as well as posterior wall (0.98±0.1, 1.15±0.1 mm; $P<0.05$, Fig 8B) thickness during systole. Additional echocardiography parameters are summarized in Table 3. Next, we quantified the scar size using Masson's Trichrome staining and observed significant reduction in scar size with ATX inhibition (11.8±2.1% vs. 20.5±3.2%, $p<0.05$; Fig 8C). This could be explained, at least in part, by the reduction in apoptotic cells in PF8380 treated mice as determined by the reduction of TUNEL positive cells 24 hours after AMI (1.5±0.3 vs. 8.9±1.3 cells per high power field, $p<0.0001$; Fig 8D). Further, we determined the capillary density in PF8380 and control mice at 7 and 30 days after AMI. ATX inhibition

was associated with a strong trend towards increased capillary density at the peri-infarct zone at 7 days (Suppl Fig 8), and this effect was significant at 30 days after AMI (60.4±5 vs. 44.3±3.8 capillaries per mm^2, $p<0.01$; Fig 8E). We did not observe significant differences between the groups in terms of body weight at 30 days after AMI (Suppl Fig 9).

4. DISCUSSION.

Acute myocardial infarction and subsequent ischemic cardiomyopathy are among the leading causes of morbidity and mortality in the United States. Prolonged post-AMI inflammatory response leads to extended monocyte and neutrophil infiltration in the injured myocardium and exacerbated myocardial damage [36]. This response has been associated with infarct expansion and impaired cardiac remodeling, thereby promoting progression to heart failure [29, 37]. While studies have documented a role for ATX/LPA signaling in the development of atherosclerosis in mice [38] and cardiovascular disease in humans [39], its role in cardiac inflammation after myocardial infarction is virtually unknown. In this study, we document, for the first time, the role of the ATX/LPA signaling nexus in the immuno-inflammatory cascade post-AMI. We demonstrate that myocardial ischemic injury enhances ATX/LPA signaling resulting in an exacerbated inflammatory response in humans and animals. Mechanistically, ATX-LPA signaling results in an exacerbated inflammatory cell production in the BM, pro-inflammatory macrophage polarization, and enhanced macrophage migration. In a gain-of-function model achieved through the deletion of LPP3, we observed an augmented inflammatory response and worsening HF post-AMI. Therapeutically, inhibition of ATX activity using clinically relevant pharmacological inhibitors reduced the inflammatory response and improved cardiac healing and functional recovery after AMI. Taken together, this is the first translational evidence of the role of ATX signaling as a mediator of post-AMI inflammation and a novel therapeutic target mitigating the ischemic cardiac damage.

We and others [10] have shown that plasma LPA levels show dynamic increase in humans after AMI; however, the mechanisms of this elevation is poorly understood. The changes in LPA level can be explained at, at least in part, by the production of DAMPs and the activation of toll-like receptor signaling [40]. Multiple reports have linked toll-like receptor activation with increased ATX expression and activity in immune cells through a type I interferon autocrine-paracrine loop involving the JAK-STAT and PI3K-Akt pathways [23]. In agreement with the literature, our data verified that AMI is associated with enhanced expression of IFNα/β and simultaneous ATX activation; corresponding with peak inflammatory response in a murine model of AMI. Mechanistically, ATX/LPA signaling exacerbates inflammation through: regulation of inflammatory cell production through its action on progenitor cell proliferation [41, 42]; polarization of monocytes/macrophages to pro-inflammatory phenotype (M1-like) [43]; and enhancement of monocytes/macrophage migration towards signals of tissue injury. Indeed, LPP3 conditional KO mice demonstrated heightened inflammatory response and BM progenitor cell proliferation post-AMI resulting in adverse cardiac remodeling and worsened cardiac function. This data was in agreement with previous human genome-wide association studies, which identify a correlation between polymorphisms that predict lower gene expression in the Plpp3 locus with an increased risk of coronary artery disease [44]. Interestingly, suppression of ATX activity reduced the post-

AMI inflammatory response and improved cardiac recovery supporting a potential therapeutic role.

Despite significant advances in timely revascularization strategies and medical therapies, millions of patients with AMI progress to develop heart failure. The innate immune response plays a major role in the sequence of events leading to this adverse response [37]. A robust body of well-designed, well-controlled foundational studies [45] conducted in humans and animal models underscores the therapeutic potential of modulating the innate immune response after AMI in enhancing cardiac recovery and tissue healing. Currently, there are no clinically approved therapies targeting post-AMI inflammation and its adverse cardiac consequences. Delayed healing and ventricular aneurysms were reported with glucocorticosteroids [46]. Similarly, non-steroidal anti-inflammatory drug use in coronary artery disease patients is associated with higher mortality and recurrent AMI [47]. Additionally, studies aimed at depleting inflammatory cells failed to demonstrate benefit [31]. In this study, we demonstrate the first evidence of a clinically relevant pharmacological therapy that specifically targets the unchecked inflammation after AMI. By inhibiting ATX activity, we are able to reduce post-AMI adverse cardiac remodeling and heart failure. The mechanism for this salutary effect appears to be related to the reduction in pro-inflammatory cytokine production such as IL-1β, which plays an important role in myelopoiesis [32, 48]. Indeed, our data suggests that PF8380 treatment reduced BM progenitor cell numbers and proliferation. The beneficial effects of reducing myelopoiesis echo recent studies targeting IL-1 in the setting of acute myocardial injury and chronic ischemic heart disease in animals and humans [49, 50]. Additionally, the reduction in expression of MCP-1 and other chemokines could explain the reduced infiltration of pro-inflammatory cells in the myocardium during the peak of inflammatory response.

There is growing interest in developing clinical pharmacological inhibitors of the ATX/LPA signaling nexus given the ubiquitous role inflammation plays in human disease. First human clinical phase II trials for idiopathic pulmonary fibrosis (IPF) using the ATX inhibitor, GLPG1690, have been successfully completed [51]. Few other inhibitors such as BMS-986020, a LPA receptor 1 antagonist and SAR100842, a LPA receptor 1 and 3 antagonist, are in phase II trials for idiopathic pulmonary fibrosis, systemic sclerosis and related fibrotic diseases [52]. Given the clinical availability of ATX inhibitors, the results of this study represent a significant step forward in the management of millions of patients with ischemic heart disease. By repurposing these therapeutics for patients with AMI, we could challenge the status quo in the management of patients with acute myocardial infarction and heart failure. Future large animal studies could test this hypothesis in translational models of acute and chronic heart failure.

Study limitations.

Our report discusses the role of ATX/LPA in post-AMI inflammation and aims at examining some of the underlying mechanisms through utilizing genetically modified mice lacking the expression of Plpp3 as well as the use of the specific ATX inhibitor, PF8380. Future mechanistic studies designed to explore the molecular and signaling mechanisms responsible for this phenomenon are currently underway. While the correlation between

ATX/LPA activation and inflammatory changes do not prove causal relationship, our data with genetic deletion of LPP3 and ATX inhibition prove the role of ATX/LPA signaling in post-AMI inflammation. The different time-course of ATX/LPA activation between human and animal studies reflect the different ischemic model (reperfusion in humans vs. permanent ligation in animal studies). The permanent LAD ligation model is ideally suited for studying cardiac functional recovery and is an excellent chronic heart failure model [53]. Moreover, the differences in the degree of cardiac remodeling in the permanent ligation model is independent of acute cardiomyocyte hypoxia injury and therefore, reflect cardiomyocyte and non-cardiomyocyte mechanisms such as inflammation, reparative and fibrotic mechanisms. Indeed, the majority of published literature has focused on the permanent ligation model due to its reproducibility, thus giving our studies clear blueprint for cross-species comparisons [36, 54, 55]. We were surprised by the enhanced angiogenesis with ATX inhibition given its well-documented role in angiogenesis [56]. However, this can be explained by the more dominant role of the anti-inflammatory effects of ATX inhibition, which could enhance the local angiogenic signal. Indeed, our *in vitro* studies demonstrated the role of PF8380 in shifting macrophages towards an anti-inflammatory phenotype, which could enhance capillary formation through the release of paracrine angiogenic factors [57]. Although ATX produces most of the systemic LPA, phospholipase D (PLD) and activated/aggregated platelets can contribute to the pool of systemic LPA which can explain why our studies demonstrate incomplete inhibition of LPA production. Our data suggest that ATX activity is enhanced in cardiac tissue after AMI which can explain the enhanced inflammatory effects. Finally, adipose tissue is an important source of circulating autotaxin and future studies examining the significance of adipose tissue in ATX/LPA signaling and post-AMI inflammation are warranted.

In conclusion, our data provides the first evidence of an important role of ATX/LPA signaling in post-AMI inflammation and the development of heart failure. Effective ATX inhibition using clinically relevant pharmacological agents in a murine model of AMI resulted in the successful modulation of the immune response and reduction in post-AMI damage and heart dysfunction. Future clinical studies targeting this novel pathway could provide successful strategies aimed at improving the outcomes of millions of patients presenting annually with acute myocardial infarction.

Supplementary Material

Refer to Web version on PubMed Central for supplementary material.

Acknowledgments

We are grateful for Jennifer Simkin for her assistance with the immunohistochemistry studies. We thank the University of Kentucky COBRE histology core for their assistance with the histological sections.

The UK Flow Cytometry & Cell Sorting core facility is supported in part by the Office of the Vice President for Research, the Markey Cancer Center and an NCI Center Core Support Grant (P30 CA177558) to the University of Kentucky Markey Cancer Center. This study used resources provided by the Lexington Veterans Affairs Medical Center.

Sources of Funding

Dr. Abdel-Latif is supported by the University of Kentucky COBRE Early Career Program (P20 GM103527) and the NIH Grant R01 HL124266. This work was supported grants from the Department of Veterans Affairs: CX001550BX001984 and CX001550 and NIH/NHLBI: HL120507 and NIGMS GM103527 to AJM and SSS.

Abbreviations.

AMI	Acute myocardial infarction
LPA	Lysophosphatidic acid
ATX	autotaxin
LPP3	Lipid phosphate phosphatase 3
Plpp3	Phospholipid phosphatase 3

REFERENCES

[1]. Nahrendorf M, Swirski FK, Aikawa E, Stangenberg L, Wurdinger T, Figueiredo JL, Libby P, Weissleder R, Pittet MJ, The healing myocardium sequentially mobilizes two monocyte subsets with divergent and complementary functions, J Exp Med 204(12) (2007) 3037–47. [PubMed: 18025128]

[2]. Sager HB, Heidt T, Hulsmans M, Dutta P, Courties G, Sebas M, Wojtkiewicz GR, Tricot B, Iwamoto Y, Sun Y, Weissleder R, Libby P, Swirski FK, Nahrendorf M, Targeting Interleukin-1beta Reduces Leukocyte Production After Acute Myocardial Infarction, Circulation 132(20) (2015) 1880–90. [PubMed: 26358260]

[3]. Nakanaga K, Hama K, Aoki J, Autotaxin--an LPA producing enzyme with diverse functions, Journal of biochemistry 148(1) (2010) 13–24. [PubMed: 20495010]

[4]. Smyth SS, Cheng HY, Miriyala S, Panchatcharam M, Morris AJ, Roles of lysophosphatidic acid in cardiovascular physiology and disease, Biochim Biophys Acta 1781(9) (2008) 563–70. [PubMed: 18586114]

[5]. Yang J, Xu J, Han X, Wang H, Zhang Y, Dong J, Deng Y, Wang J, Lysophosphatidic Acid Is Associated With Cardiac Dysfunction and Hypertrophy by Suppressing Autophagy via the LPA3/AKT/mTOR Pathway, Frontiers in physiology 9 (2018) 1315. [PubMed: 30283359]

[6]. Panchatcharam M, Miriyala S, Salous A, Wheeler J, Dong A, Mueller P, Sunkara M, Escalante-Alcalde D, Morris AJ, Smyth SS, Lipid phosphate phosphatase 3 negatively regulates smooth muscle cell phenotypic modulation to limit intimal hyperplasia, Arterioscler Thromb Vasc Biol 33(1) (2013) 52–9. [PubMed: 23104851]

[7]. Panchatcharam M, Salous AK, Brandon J, Miriyala S, Wheeler J, Patil P, Sunkara M, Morris AJ, Escalante-Alcalde D, Smyth SS, Mice with targeted inactivation of ppap2b in endothelial and hematopoietic cells display enhanced vascular inflammation and permeability, Arterioscler Thromb Vasc Biol 34(4) (2014) 837–45. [PubMed: 24504738]

[8]. Zhou Z, Subramanian P, Sevilmis G, Globke B, Soehnlein O, Karshovska E, Megens R, Heyll K, Chun J, Saulnier-Blache JS, Reinholz M, van Zandvoort M, Weber C, Schober A, Lipoprotein-derived lysophosphatidic acid promotes atherosclerosis by releasing CXCL1 from the endothelium, Cell Metab 13(5) (2011) 592–600. [PubMed: 21531341]

[9]. Smyth SS, Mueller P, Yang F, Brandon JA, Morris AJ, Arguing the case for the autotaxin-lysophosphatidic acid-lipid phosphate phosphatase 3-signaling nexus in the development and complications of atherosclerosis, Arterioscler Thromb Vasc Biol 34(3) (2014) 479–86. [PubMed: 24482375]

[10]. Chen X, Yang XY, Wang ND, Ding C, Yang YJ, You ZJ, Su Q, Chen JH, Serum lysophosphatidic acid concentrations measured by dot immunogold filtration assay in patients with acute myocardial infarction, Scand J Clin Lab Invest 63(7–8) (2003) 497–503. [PubMed: 14743959]

[11]. Escalante-Alcalde D, Morales SL, Stewart CL, Generation of a reporter-null allele of Ppap2b/Lpp3and its expression during embryogenesis, The International journal of developmental biology 53(1) (2009) 139–47. [PubMed: 19123136]

[12]. Ramos-Perez WD, Fang V, Escalante-Alcalde D, Cammer M, Schwab SR, A map of the distribution of sphingosine 1-phosphate in the spleen, Nat Immunol 16(12) (2015) 1245–52. [PubMed: 26502404]

[13]. Shih DM, Zhu W, Schugar RC, Meng Y, Jia X, Miikeda A, Wang Z, Zieger M, Lee R, Graham M, Allayee H, Cantor RM, Mueller C, Brown JM, Hazen SL, Lusis AJ, Genetic Deficiency of Flavin-Containing Monooxygenase 3 (Fmo3) Protects Against Thrombosis but Has Only a Minor Effect on Plasma Lipid Levels-Brief Report, Arterioscler Thromb Vasc Biol 39(6) (2019) 1045–1054. [PubMed: 31070450]

[14]. Gao E, Lei YH, Shang X, Huang ZM, Zuo L, Boucher M, Fan Q, Chuprun JK, Ma XL, Koch WJ, A novel and efficient model of coronary artery ligation and myocardial infarction in the mouse, Circ Res 107(12) (2010) 1445–53. [PubMed: 20966393]

[15]. Gierse J, Thorarensen A, Beltey K, Bradshaw-Pierce E, Cortes-Burgos L, Hall T, Johnston A, Murphy M, Nemirovskiy O, Ogawa S, Pegg L, Pelc M, Prinsen M, Schnute M, Wendling J, Wene S, Weinberg R, Wittwer A, Zweifel B, Masferrer J, A novel autotaxin inhibitor reduces lysophosphatidic acid levels in plasma and the site of inflammation, J Pharmacol Exp Ther 334(1) (2010) 310–7. [PubMed: 20392816]

[16]. Klyachkin YM, Nagareddy PR, Ye S, Wysoczynski M, Asfour A, Gao E, Sunkara M, Brandon JA, Annabathula R, Ponnapureddy R, Solanki M, Pervaiz ZH, Smyth SS, Ratajczak MZ, Morris AJ, Abdel-Latif A, Pharmacological Elevation of Circulating Bioactive Phosphosphingolipids Enhances Myocardial Recovery After Acute Infarction, Stem Cells Transl Med 4(11) (2015) 1333–43. [PubMed: 26371341]

[17]. Salous AK, Panchatcharam M, Sunkara M, Mueller P, Dong A, Wang Y, Graf GA, Smyth SS, Morris AJ, Mechanism of rapid elimination of lysophosphatidic acid and related lipids from the circulation of mice, J Lipid Res 54(10) (2013) 2775–84. [PubMed: 23948545]

[18]. Wang CY, Liao JK, A mouse model of diet-induced obesity and insulin resistance, Methods in molecular biology (Clifton, N.J.) 821 (2012) 421–33.

[19]. Zhang D, Zhang Y, Zhao C, Zhang W, Shao G, Zhang H, Effect of lysophosphatidic acid on the immune inflammatory response and the connexin 43 protein in myocardial infarction, Experimental and therapeutic medicine 11(5) (2016) 1617–1624. [PubMed: 27168781]

[20]. Bouchareb R, Mahmut A, Nsaibia MJ, Boulanger MC, Dahou A, Lepine JL, Laflamme MH, Hadji F, Couture C, Trahan S, Page S, Bosse Y, Pibarot P, Scipione CA, Romagnuolo R, Koschinsky ML, Arsenault BJ, Marette A, Mathieu P, Autotaxin Derived From Lipoprotein(a) and Valve Interstitial Cells Promotes Inflammation and Mineralization of the Aortic Valve, Circulation 132(8) (2015) 677–90. [PubMed: 26224810]

[21]. Shantsila E, Wrigley B, Tapp L, Apostolakis S, Montoro-Garcia S, Drayson MT, Lip GY, Immunophenotypic characterization of human monocyte subsets: possible implications for cardiovascular disease pathophysiology, Journal of thrombosis and haemostasis : JTH 9(5) (2011) 1056–66. [PubMed: 21342432]

[22]. Christia P, Frangogiannis NG, Targeting inflammatory pathways in myocardial infarction, European journal of clinical investigation 43(9) (2013) 986–95. [PubMed: 23772948]

[23]. Song J, Guan M, Zhao Z, Zhang J, Type I Interferons Function as Autocrine and Paracrine Factors to Induce Autotaxin in Response to TLR Activation, PLoS One 10(8) (2015) e0136629. [PubMed: 26313906]

[24]. Park GY, Lee YG, Berdyshev E, Nyenhuis S, Du J, Fu P, Gorshkova IA, Li Y, Chung S, Karpurapu M, Deng J, Ranjan R, Xiao L, Jaffe HA, Corbridge SJ, Kelly EA, Jarjour NN, Chun J, Prestwich GD, Kaffe E, Ninou I, Aidinis V, Morris AJ, Smyth SS, Ackerman SJ, Natarajan V, Christman JW, Autotaxin production of lysophosphatidic acid mediates allergic asthmatic inflammation, Am J Respir Crit Care Med 188(8) (2013) 928–40. [PubMed: 24050723]

[25]. Benesch MGK, MacIntyre ITK, McMullen TPW, Brindley DN, Coming of Age for Autotaxin and Lysophosphatidate Signaling: Clinical Applications for Preventing, Detecting and Targeting Tumor-Promoting Inflammation, Cancers (Basel) 10(3) (2018).

[26]. Lavine KJ, Epelman S, Uchida K, Weber KJ, Nichols CG, Schilling JD, Ornitz DM, Randolph GJ, Mann DL, Distinct macrophage lineages contribute to disparate patterns of cardiac recovery and remodeling in the neonatal and adult heart, Proc Natl Acad Sci U S A 111(45) (2014) 16029–34. [PubMed: 25349429]

[27]. Annamalai L, Westmoreland SV, Domingues HG, Walsh DG, Gonzalez RG, O'Neil SP, Myocarditis in CD8-depleted SIV-infected rhesus macaques after short-term dual therapy with nucleoside and nucleotide reverse transcriptase inhibitors, PLoS One 5(12) (2010) e14429. [PubMed: 21203448]

[28]. Maekawa Y, Anzai T, Yoshikawa T, Asakura Y, Takahashi T, Ishikawa S, Mitamura H, Ogawa S, Prognostic significance of peripheral monocytosis after reperfused acute myocardial infarction:a possible role for left ventricular remodeling, J Am Coll Cardiol 39(2) (2002) 241–6. [PubMed: 11788214]

[29]. Panizzi P, Swirski FK, Figueiredo JL, Waterman P, Sosnovik DE, Aikawa E, Libby P, Pittet M, Weissleder R, Nahrendorf M, Impaired infarct healing in atherosclerotic mice with Ly-6C(hi) monocytosis, J Am Coll Cardiol 55(15) (2010) 1629–38. [PubMed: 20378083]

[30]. Weng J, Jiang S, Ding L, Xu Y, Zhu X, Jin P, Autotaxin/lysophosphatidic acid signaling mediates obesity-related cardiomyopathy in mice and human subjects, Journal of cellular and molecular medicine 23(2) (2019) 1050–1058. [PubMed: 30450805]

[31]. Horckmans M, Ring L, Duchene J, Santovito D, Schloss MJ, Drechsler M, Weber C, Soehnlein O, Steffens S, Neutrophils orchestrate post-myocardial infarction healing by polarizing macrophages towards a reparative phenotype, Eur Heart J 38(3) (2017) 187–197. [PubMed: 28158426]

[32]. Nagareddy PR, Kraakman M, Masters SL, Stirzaker RA, Gorman DJ, Grant RW, Dragoljevic D, Hong ES, Abdel-Latif A, Smyth SS, Choi SH, Korner J, Bornfeldt KE, Fisher EA, Dixit VD, Tall AR, Goldberg IJ, Murphy AJ, Adipose tissue macrophages promote myelopoiesis and monocytosis in obesity, Cell metabolism 19(5) (2014) 821–35. [PubMed: 24807222]

[33]. Gensel JC, Kopper TJ, Zhang B, Orr MB, Bailey WM, Predictive screening of M1 and M2 macrophages reveals the immunomodulatory effectiveness of post spinal cord injury azithromycin treatment, Sci Rep 7 (2017) 40144. [PubMed: 28057928]

[34]. Hu J, Huang CX, Rao PP, Zhou JP, Wang X, Tang L, Liu MX, Zhang GG, Inhibition of microRNA-155 attenuates sympathetic neural remodeling following myocardial infarction via reducing M1 macrophage polarization and inflammatory responses in mice, European journal of pharmacology 851 (2019) 122–132. [PubMed: 30721702]

[35]. Haydar D, Cory TJ, Birket SE, Murphy BS, Pennypacker KR, Sinai AP, Feola DJ, Azithromycin Polarizes Macrophages to an M2 Phenotype via Inhibition of the STAT1 and NF-kappaB Signaling Pathways, J Immunol 203(4) (2019) 1021–1030. [PubMed: 31263039]

[36]. Epelman S, Liu PP, Mann DL, Role of innate and adaptive immune mechanisms in cardiac injury and repair, Nat Rev Immunol 15(2) (2015) 117–29. [PubMed: 25614321]

[37]. Zouggari Y, Ait-Oufella H, Bonnin P, Simon T, Sage AP, Guerin C, Vilar J, Caligiuri G, Tsiantoulas D, Laurans L, Dumeau E, Kotti S, Bruneval P, Charo IF, Binder CJ, Danchin N, Tedgui A, Tedder TF, Silvestre JS, Mallat Z, B lymphocytes trigger monocyte mobilization and impair heart function after acute myocardial infarction, Nat Med 19(10) (2013) 1273–80. [PubMed: 24037091]

[38]. Mueller P, Ye S, Morris A, Smyth SS, Lysophospholipid mediators in the vasculature, Exp Cell Res 333(2) (2015) 190–4. [PubMed: 25825155]

[39]. Reschen ME, Gaulton KJ, Lin D, Soilleux EJ, Morris AJ, Smyth SS, O'Callaghan CA, Lipid-induced epigenomic changes in human macrophages identify a coronary artery disease-associated variant that regulates PPAP2B Expression through Altered C/EBP-beta binding, PLoS Genet 11(4) (2015) e1005061. [PubMed: 25835000]

[40]. Sreejit G, Abdel-Latif A, Athmanathan B, Annabathula R, Dhyani A, Noothi SK, Quaife-Ryan GA, Al-Sharea A, Pernes G, Dragoljevic D, Lal H, Schroder K, Hanaoka BY, Raman C, Grant MB, Hudson JE, Smyth SS, Porrello ER, Murphy AJ, Nagareddy PR, Neutrophil-Derived S100A8/A9 Amplify Granulopoiesis After Myocardial Infarction, Circulation 141(13) (2020) 1080–1094. [PubMed: 31941367]

[41]. Evseenko D, Latour B, Richardson W, Corselli M, Sahaghian A, Cardinal S, Zhu Y, Chan R, Dunn B, Crooks GM, Lysophosphatidic acid mediates myeloid differentiation within the human bone marrow microenvironment, PLoS One 8(5) (2013) e63718. [PubMed: 23696850]

[42]. Igarashi H, Akahoshi N, Ohto-Nakanishi T, Yasuda D, Ishii S, The lysophosphatidic acid receptor LPA4 regulates hematopoiesis-supporting activity of bone marrow stromal cells, Sci Rep 5 (2015) 11410. [PubMed: 26090649]

[43]. Qin X, Qiu C, Zhao L, Lysophosphatidylcholine perpetuates macrophage polarization toward classically activated phenotype in inflammation, Cell Immunol 289(1–2) (2014) 185–90. [PubMed: 24841857]

[44]. Deloukas P, Kanoni S, Willenborg C, Farrall M, Assimes TL, Thompson JR, Ingelsson E, Saleheen D, Erdmann J, Goldstein BA, Stirrups K, Konig IR, Cazier JB, Johansson A, Hall AS, Lee JY, Willer CJ, Chambers JC, Esko T, Folkersen L, Goel A, Grundberg E, Havulinna AS, Ho WK, Hopewell JC, Eriksson N, Kleber ME, Kristiansson K, Lundmark P, Lyytikainen LP, Rafelt S, Shungin D, Strawbridge RJ, Thorleifsson G, Tikkanen E, Van Zuydam N, Voight BF, Waite LL, Zhang W, Ziegler A, Absher D, Altshuler D, Balmforth AJ, Barroso I, Braund PS, Burgdorf C, Claudi-Boehm S, Cox D, Dimitriou M, Do R, Doney AS, El Mokhtari N, Eriksson P, Fischer K, Fontanillas P, Franco-Cereceda A, Gigante B, Groop L, Gustafsson S, Hager J, Hallmans G, Han BG, Hunt SE, Kang HM, Illig T, Kessler T, Knowles JW, Kolovou G, Kuusisto J, Langenberg C, Langford C, Leander K, Lokki ML, Lundmark A, McCarthy MI, Meisinger C, Melander O, Mihailov E, Maouche S, Morris AD, Muller-Nurasyid M, Nikus K, Peden JF, Rayner NW, Rasheed A, Rosinger S, Rubin D, Rumpf MP, Schafer A, Sivananthan M, Song C, Stewart AF, Tan ST, Thorgeirsson G, van der Schoot CE, Wagner PJ, Wells GA, Wild PS, Yang TP, Amouyel P, Arveiler D, Basart H, Boehnke M, Boerwinkle E, Brambilla P, Cambien F, Cupples AL, de Faire U, Dehghan A, Diemert P, Epstein SE, Evans A, Ferrario MM, Ferrieres J, Gauguier D, Go AS, Goodall AH, Gudnason V, Hazen SL, Holm H, Iribarren C, Jang Y, Kahonen M, Kee F, Kim HS, Klopp N, Koenig W, Kratzer W, Kuulasmaa K, Laakso M, Laaksonen R, Lee JY, Lind L, Ouwehand WH, Parish S, Park JE, Pedersen NL, Peters A, Quertermous T, Rader DJ, Salomaa V, Schadt E, Shah SH, Sinisalo J, Stark K, Stefansson K, Tregouet DA, Virtamo J, Wallentin L, Wareham N, Zimmermann ME, Nieminen MS, Hengstenberg C, Sandhu MS, Pastinen T, Syvanen AC, Hovingh GK, Dedoussis G, Franks PW, Lehtimaki T, Metspalu A, Zalloua PA, Siegbahn A, Schreiber S, Ripatti S, Blankenberg SS, Perola M, Clarke R, Boehm BO, O'Donnell C, Reilly MP, Marz W, Collins R, Kathiresan S, Hamsten A, Kooner JS, Thorsteinsdottir U, Danesh J, Palmer CN, Roberts R, Watkins H, Schunkert H, Samani NJ, Large-scale association analysis identifies new risk loci for coronary artery disease, Nature genetics 45(1) (2013) 25–33. [PubMed: 23202125]

[45]. Frangogiannis NG, The inflammatory response in myocardial injury, repair, and remodelling, Nat Rev Cardiol 11(5) (2014) 255–65. [PubMed: 24663091]

[46]. Bulkley BH, Roberts WC, Steroid therapy during acute myocardial infarction. A cause of delayed healing and of ventricular aneurysm, Am J Med 56(2) (1974) 244–50. [PubMed: 4812079]

[47]. Schjerning Olsen AM, Fosbol EL, Lindhardsen J, Folke F, Charlot M, Selmer C, Lamberts M, Bjerring Olesen J, Kober L, Hansen PR, Torp-Pedersen C, Gislason GH, Duration of treatment with nonsteroidal anti-inflammatory drugs and impact on risk of death and recurrent myocardial infarction in patients with prior myocardial infarction: a nationwide cohort study, Circulation 123(20) (2011) 2226–35. [PubMed: 21555710]

[48]. Hsu LC, Enzler T, Seita J, Timmer AM, Lee CY, Lai TY, Yu GY, Lai LC, Temkin V, Sinzig U, Aung T, Nizet V, Weissman IL, Karin M, IL-1beta-driven neutrophilia preserves antibacterial defense in the absence of the kinase IKKbeta, Nature immunology 12(2) (2011) 144–50. [PubMed: 21170027]

[49]. Abbate A, Morton AC, Crossman DC, Anti-inflammatory therapies in myocardial infarction, Lancet 385(9987) (2015) 2573–4.

[50]. Ridker PM, Everett BM, Thuren T, MacFadyen JG, Chang WH, Ballantyne C, Fonseca F, Nicolau J, Koenig W, Anker SD, Kastelein JJP, Cornel JH, Pais P, Pella D, Genest J, Cifkova R, Lorenzatti A, Forster T, Kobalava Z, Vida-Simiti L, Flather M, Shimokawa H, Ogawa H, Dellborg M, Rossi PRF, Troquay RPT, Libby P, Glynn RJ, Group CT, Antiinflammatory Therapy with Canakinumab for Atherosclerotic Disease, N Engl J Med 377(12) (2017) 1119–1131. [PubMed: 28845751]

[51]. Maher TM, van der Aar EM, Van de Steen O, Allamassey L, Desrivot J, Dupont S, Fagard L, Ford P, Fieuw A, Wuyts W, Safety, tolerability, pharmacokinetics, and pharmacodynamics of GLPG1690, a novel autotaxin inhibitor, to treat idiopathic pulmonary fibrosis (FLORA): a phase 2a randomised placebo-controlled trial, The Lancet. Respiratory medicine 6(8) (2018) 627–635. [PubMed: 29792287]

[52]. Kihara Y, Mizuno H, Chun J, Lysophospholipid receptors in drug discovery, Experimental cell research 333(2) (2015) 171–7. [PubMed: 25499971]

[53]. Lindsey ML, Bolli R, Canty JM Jr., Du XJ, Frangogiannis NG, Frantz S, Gourdie RG, Holmes JW, Jones SP, Kloner RA, Lefer DJ, Liao R, Murphy E, Ping P, Przyklenk K, Recchia FA, Schwartz Longacre L, Ripplinger CM, Van Eyk JE, Heusch G, Guidelines for experimental models of myocardial ischemia and infarction, Am J Physiol Heart Circ Physiol 314(4) (2018) H812–H838. [PubMed: 29351451]

[54]. Dick SA, Macklin JA, Nejat S, Momen A, Clemente-Casares X, Althagafi MG, Chen J, Kantores C, Hosseinzadeh S, Aronoff L, Wong A, Zaman R, Barbu I, Besla R, Lavine KJ, Razani B, Ginhoux F, Husain M, Cybulsky MI, Robbins CS, Epelman S, Self-renewing resident cardiac macrophages limit adverse remodeling following myocardial infarction, Nat Immunol 20(1) (2019) 29–39. [PubMed: 30538339]

[55]. Nahrendorf M, Pittet MJ, Swirski FK, Monocytes: protagonists of infarct inflammation and repair after myocardial infarction, Circulation 121(22) (2010) 2437–45. [PubMed: 20530020]

[56]. Ptaszynska MM, Pendrak ML, Stracke ML, Roberts DD, Autotaxin signaling via lysophosphatidic acid receptors contributes to vascular endothelial growth factor-induced endothelial cell migration, Molecular cancer research : MCR 8(3) (2010) 309–21. [PubMed: 20197381]

[57]. Al-Darraji A, Haydar D, Chelvarajan L, Tripathi H, Levitan B, Gao E, Venditto VJ, Gensel JC, Feola DJ, Abdel-Latif A, Azithromycin therapy reduces cardiac inflammation and mitigates adverse cardiac remodeling after myocardial infarction: Potential therapeutic targets in ischemic heart disease, PLoS One 13(7) (2018) e0200474. [PubMed: 30001416]

HIGHLIGHTS

- LPA-ATX signaling nexus modulated post-myocardial infarction inflammation.
- Pharmacological inhibition of ATX/LPA signaling attenuates cardiac and systemic inflammation after ischemic myocardial injury.
- ATX inhibition after acute myocardial infraction enhances cardiac recovery, reduces adverse remodeling and scar size post-infraction.

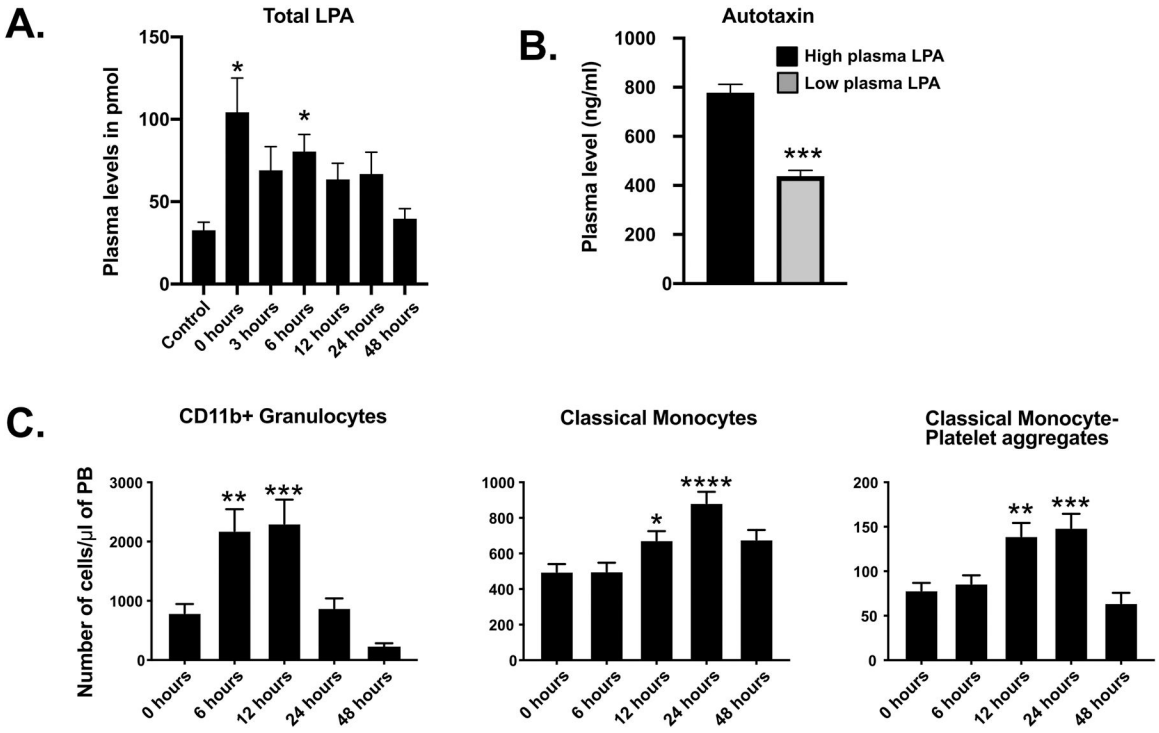

Figure 1. LPA, autotaxin and inflammatory cell number increased in AMI patients.

PB samples were collected from ST-elevation myocardial infraction patients at time of presentation to the hospital (0 hours), then 3,6,12 and 24 hours after myocardial infarction and 5 matched controls. **(A)** Mass spectrometry analysis of plasma LPA demonstrate elevated levels at the early time points after acute injury compared to matched controls (levels presented as pmol). **(B)** ELISA analysis of ATX concentration in patients with high (above median) and low (below median) plasma LPA levels showing significantly higher activity among patients with plasma LPA level above median. **(C)** Granulocytes and classical monocytes expressing CD11b demonstrated dynamic changes after myocardial infarction with a peak between 3 and 12 hours after injury. Comparison between groups was performed by Student *t*-test or repeated measures ANOVA, *$P \leq 0.05$, **$p \leq 0.01$, ***$P \leq 0.001$, ****$P \leq 0.0001$. Values are presented as mean ±SEM. ATX, autotaxin; LPA, lysophosphatidic acid; PBMCs, peripheral blood mononuclear cells.

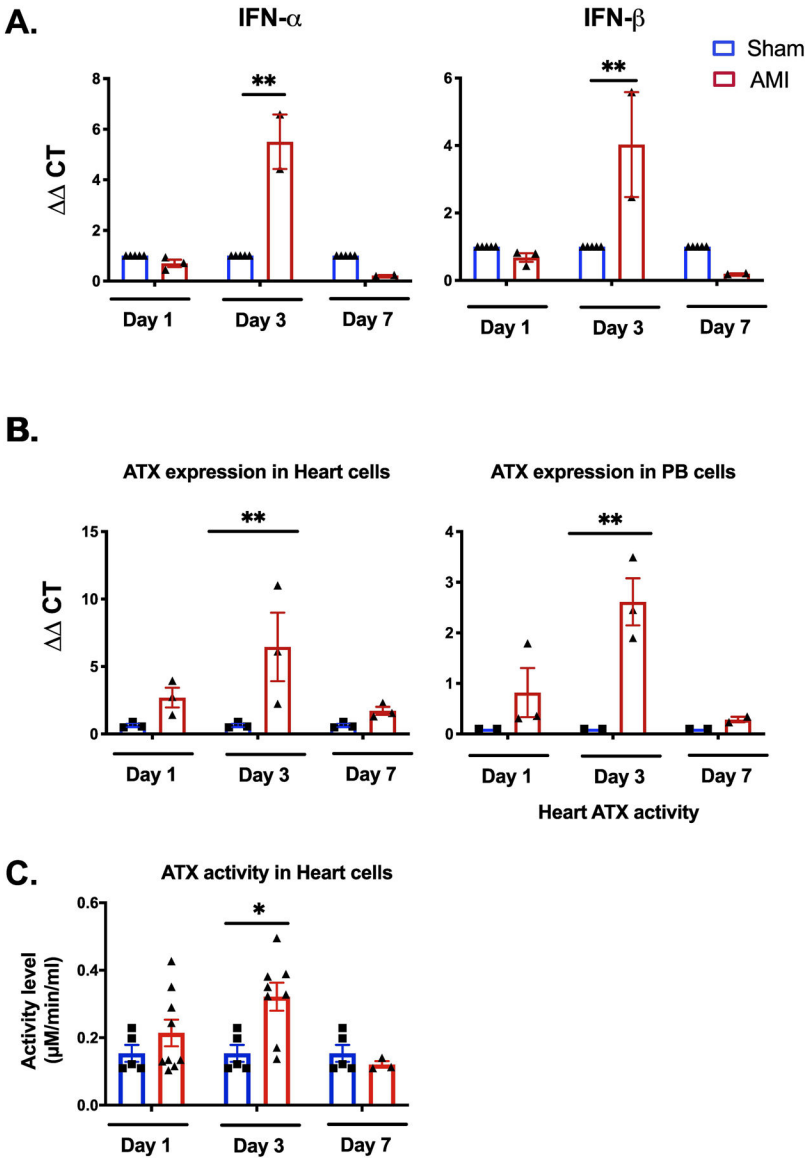

Figure 2. IFN-α, IFN-β and ATX expression increased in heart and peripheral blood after AMI.

(A) 8–10 week old female C57BL/6 mice, underwent LAD ligation or SHAM surgery. The expression of IFN-α and IFN-β in cardiac tissue was significantly higher on day 3 in comparison to other time points and sham operated mice **(B)** The expression of autotaxin in cardiac tissue and peripheral blood cells corresponded to that of IFN's and peaked at 3 days after ischemic injury (n=3 mice/group/time-point). **(C)** The activity of ATX corelated with the gene expression in cardiac tissue after AMI peaking at day 3. Comparison between groups was performed by repeated measures ANOVA, $*P \leq 0.05$, $**P \leq 0.01$ ATX, autotaxin; IFN-α, Interferon-α; IFN-β, Interferon-β.

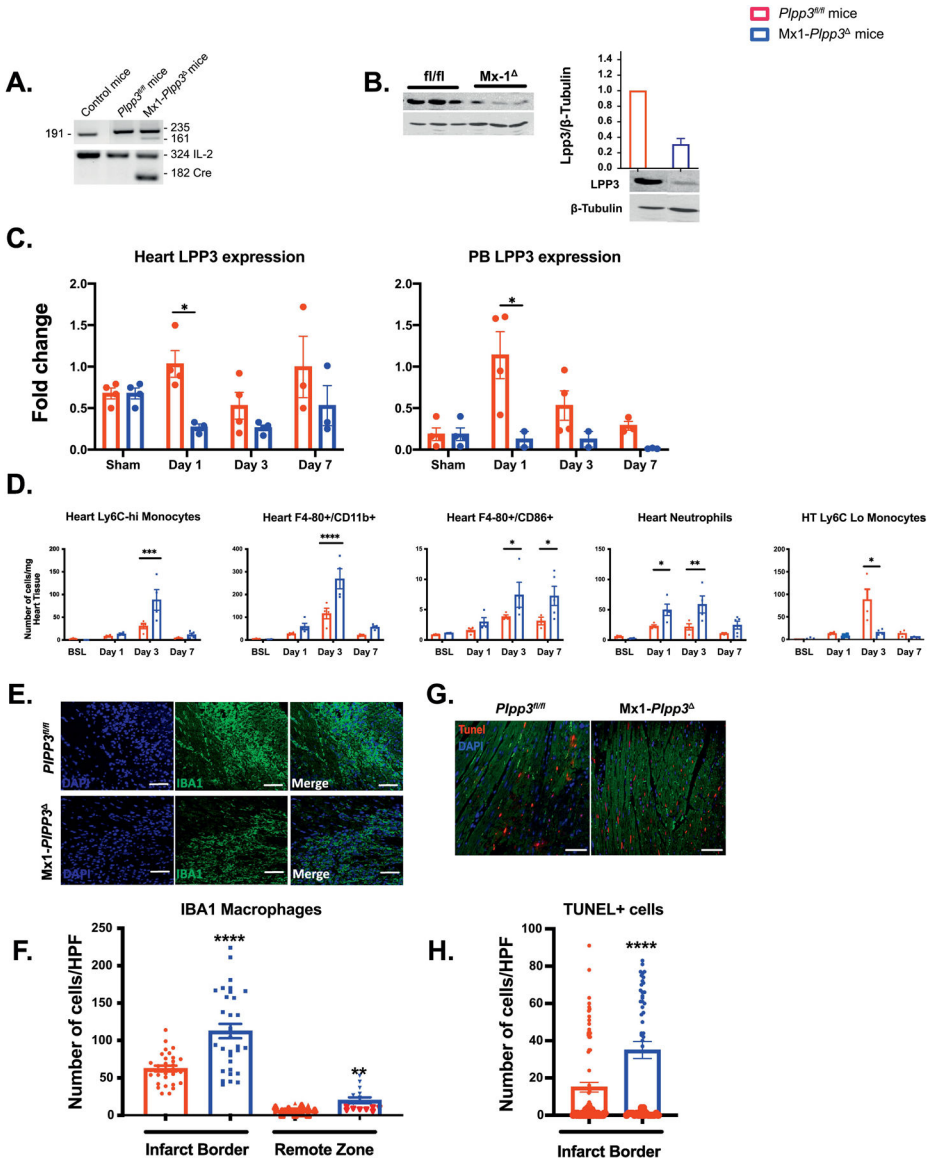

Figure 3. Global LPP3 deletion is associated with exacerbated inflammatory response following acute myocardial ischemia.

Mx1- Plpp3$^{\Delta}$ and Plpp3$^{fl/fl}$ LPP3 KO mice were subjected to myocardial infarction followed by assessment of inflammatory response at days 1, 3 and 7 after injury. **(A)** shows PCR screening for the totally recombined allele, loxP present is 235 bp (Plpp3$^{fl/fl}$), and excision of LPP3 is 161 bp (Mx1- Plpp3$^{\Delta}$). **(B)** Western blotting demonstrates LPP3 protein expression in Plpp3$^{fl/fl}$ and Mx1- Plpp3$^{\Delta}$ with β- tubulin used as a loading control. LPP3 expression was normalized to β-tubulin staining (n = 3 animals) and presented as mean±SD in which the density of Lpp3 in the Plpp3$^{fl/fl}$ samples was set to 1. **(C)** The expression of LPP3 in cardiac tissue and peripheral blood cells showed elevation after AMI but this effect was attenuated in Mx1- Plpp3$^{\Delta}$ in comparison to Plpp3$^{fl/fl}$ at all the time points after ischemic injury (n=3 mice/group/time-point). **(D)** Flow cytometry analysis of cardiac inflammatory cells showed elevated Ly6C^{hi} monocytes (CD45^{+}/Ly6C/G^{hi}/CD115^{hi}), pro-inflammatory macrophages (CD45^{+}/F4-80^{+}/CD11b^{+}) and (CD45^{+}/F4-80^{+}/CD86^{+}) and

neutrophils ($CD45^{+}/CD115^{lo}/Ly6G/C^{lo}$),in Mx1- $Plpp3^{\Delta}$ mice peaking 3 days after myocardial infraction. On the other hand, there was significantly lower number of anti-inflammatory monocytes in Mx1- $Plpp3^{\Delta}$ mice. **(E)** Immunohistochemical assessment of macrophages based on the expression of IBA1 (green) in the heart section post MI on day 3. **(F)** Quantitative analysis of IBA1 in infract border and remote zone showed significantly high number of IBA in Mx1- $Plpp3^{\Delta}$ mice compared to littermate controls (n=4 mice/group/time-point). **(G)** Immunohistochemical assessment of TUNEL staining (red) in the heart section post AMI on day 3. **(H)** Quantitative analysis of TUNEL positive cells in infract border showed significantly higher number of apoptotic cells in Mx1-$Plpp3^{\Delta}$ mice compared to littermate controls (n=4 mice/group/time-point). Comparison between groups was performed by repeated measures ANOVA [Panel C] or Student *t*-test [Panels E and G] $*P \leq 0.05$, $**P \leq 0.01$, $***P \leq 0.001$, $****P \leq 0.0001$ HPF: high power field; LPP3, Lipid phosphate phosphatase3. Scale bars represent 50 μm

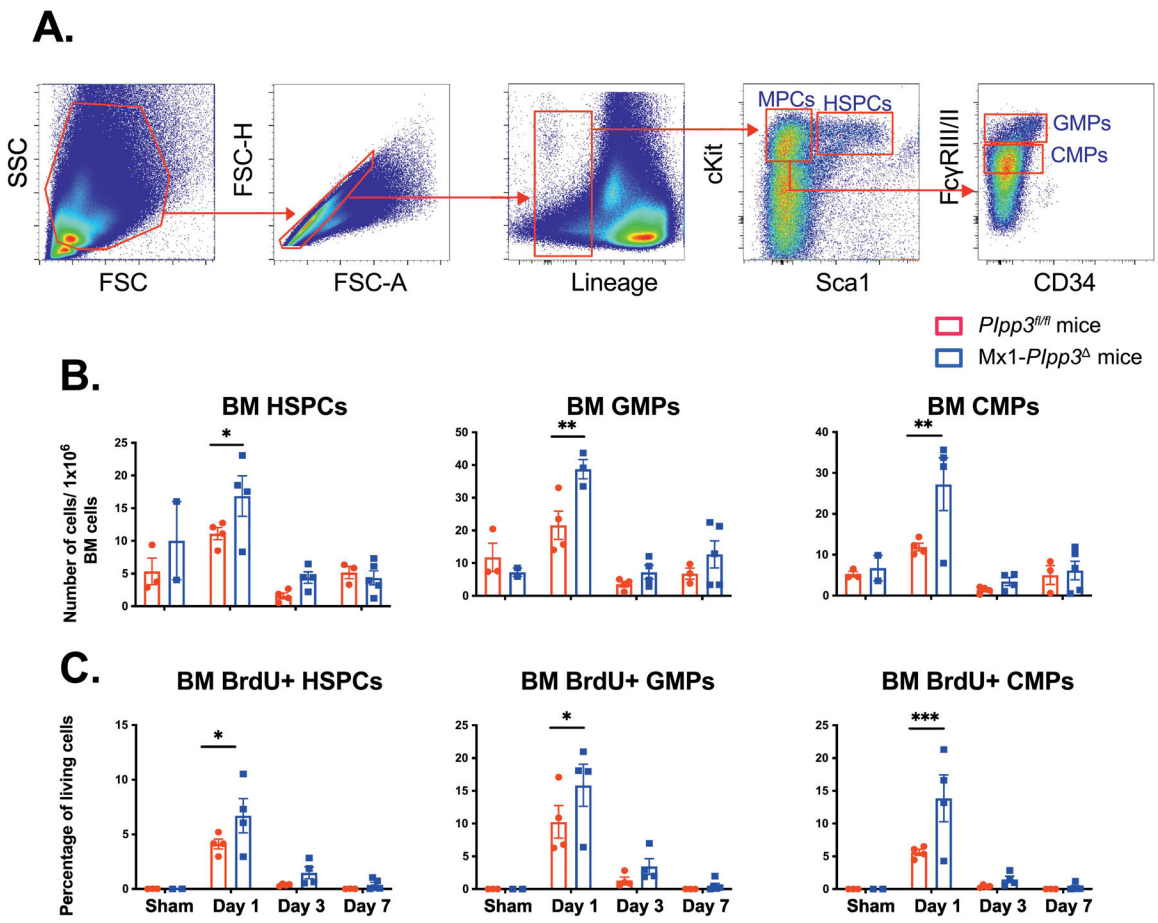

Figure 4. Leukocytosis in Mx1- Plpp3$^{\Delta}$ mice post-AMI is due to increased number and proliferation of bone marrow progenitor cells:

(A) Flow cytometric plots demonstrating the gating strategy for hematopoietic stem progenitor cells (Sca-1^{-}/c-Kit^{+}/ Lin^{-}), common myeloid progenitors (Lin^{-}/c-Kit^{+}/Sca-1^{-} CD16/32^{-}/CD34^{+}) and granulocyte macrophage progenitors (Lin^{-} c-Kit^{+}/Sca-1^{-}/CD16/32^{+}/ CD34^{+}) in the bone marrow. **(B,C)** Flow cytometry analyses of hematopoietic progenitor number and percentage of BrdU^{+} cells showing a significant increase in number and proliferation of HSPCs, CMPs and GMPs in the bone marrow from Mx1- Plpp3$^{\Delta}$ mice compared to littermate Plpp3$^{fl/fl}$ controls (n=4 mice/group/time-point). Comparison between groups was performed by repeated measures ANOVA, *$P \leq 0.05$, **$P \leq 0.01$, ***$P \leq 0.001$ BM, bone marrow; BrdU, Bromodeoxyuridine/5-bromo-2'-deoxyuridine; CMP: Common myeloid progenitors; GMP, Granulocyte macrophage progenitors; HSPCS; Hematopoietic stem progenitor cells.

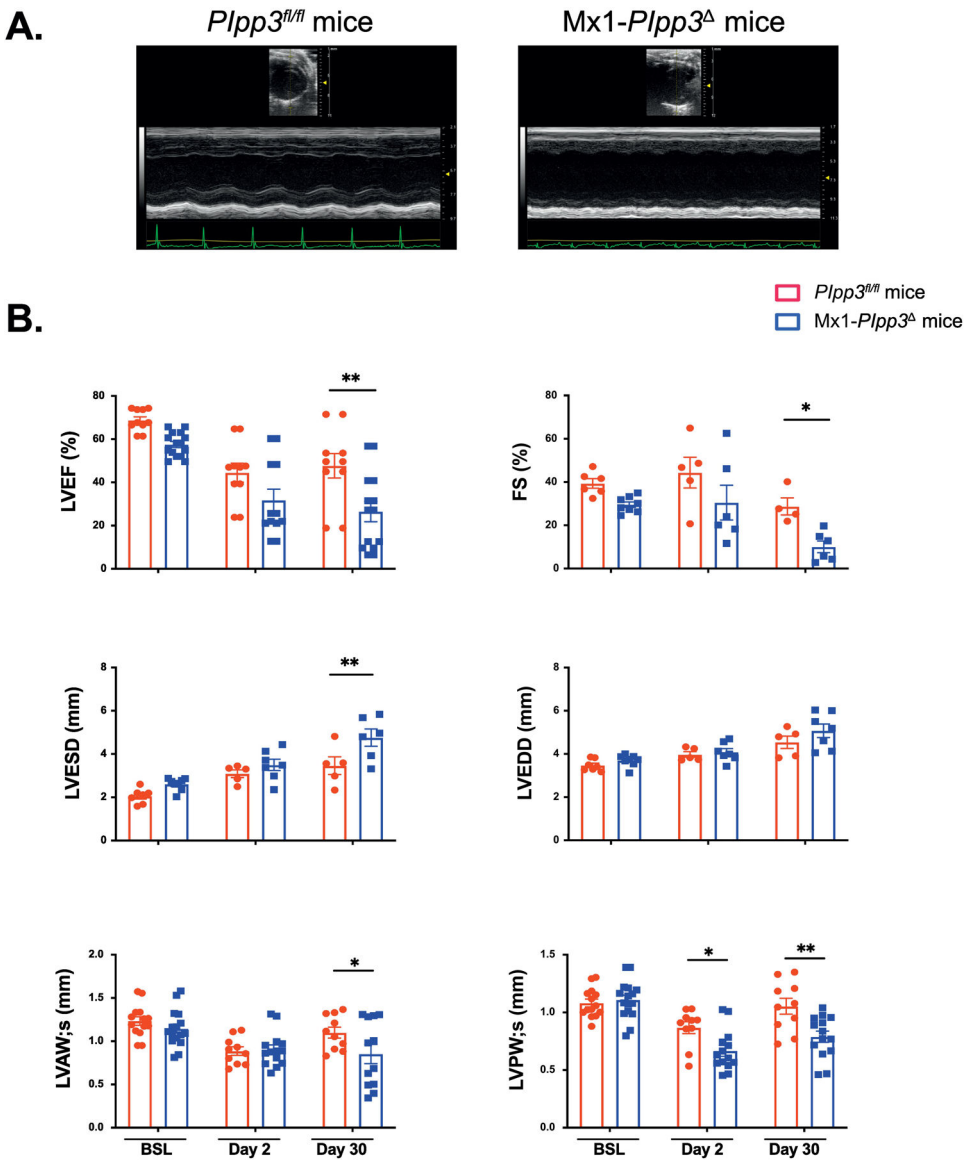

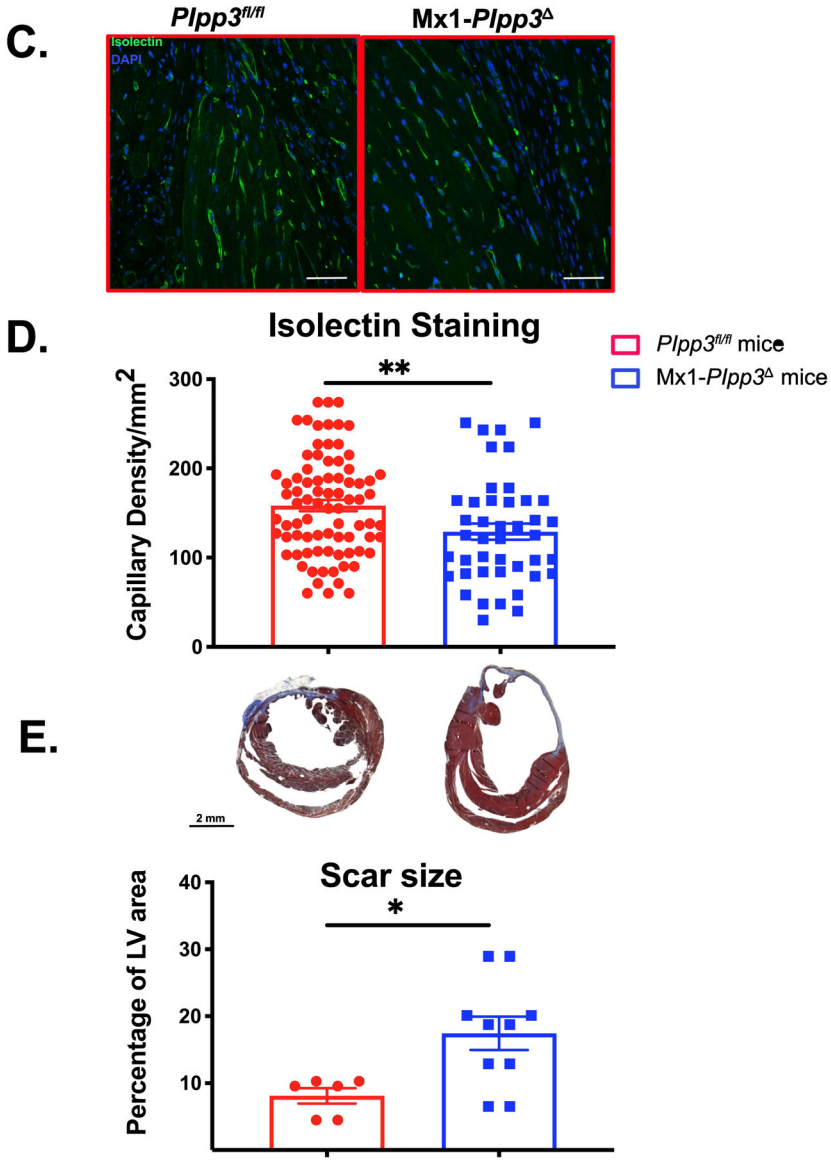

Figure 5. Mx1- Plpp3$^{\Delta}$ mice showed greater deterioration in cardiac function, large scar size and attenuated angiogenesis after myocardial injury.

(A) 30 day following AMI, transthoracic echocardiography using M-Mode and 2D echocardiography was performed on Mx1- Plpp3$^{\Delta}$ and Plpp3$^{fl/fl}$ mice to evaluate left ventricular function and remodeling parameters. **(B)** Quantitative analyses of M-mode and 2D echocardiography demonstrate significant reduction in LV function as assessed by left ventricular ejection fraction and fractional shortening. Similarly, Mx1- Plpp3$^{\Delta}$ exhibited greater deterioration in parameters of left ventricular remodeling such as left ventricular end-systolic and end-diastolic diameters. **(C)** Representative isolectin staining (green) image for capillary density in the peri-infarct region in Mx1- Plpp3$^{\Delta}$ and Plpp3$^{fl/fl}$ mice demonstrates lower capillary density in Mx1- Plpp3$^{\Delta}$ mice. **(D)** Quantitative analysis of capillary density confirms the reduced angiogenesis and capillary density in Mx1- Plpp3$^{\Delta}$ mice Scale bars represent 50 μm **(E)** Representative picture shows Masson's trichrome staining done at 30 days after LAD ligation. Quantitative analysis of scar size as percentage of left ventricular

area showed significant increase in scar size in Mx1- Plpp3$^{\Delta}$ mice compared to Plpp3$^{fl/fl}$ controls. (n=5 mice/group/time-point). Comparison between groups was performed by repeated measures ANOVA, *$P \leq 0.05$, **$P \leq 0.01$, ****$P < 0.001$. AMI, Acute myocardial infarction; FS, fractional shortening; LAD, left anterior descending artery; LV, left ventricular; LVAWs, left ventricular anterior wall thickness in systole; LVEF, left ventricular ejection fraction; LVEDD, left ventricular end-diastolic diameter; LVESD, left ventricular end-systolic diameter; LVPWs, left ventricular posterior wall thickness in systole.

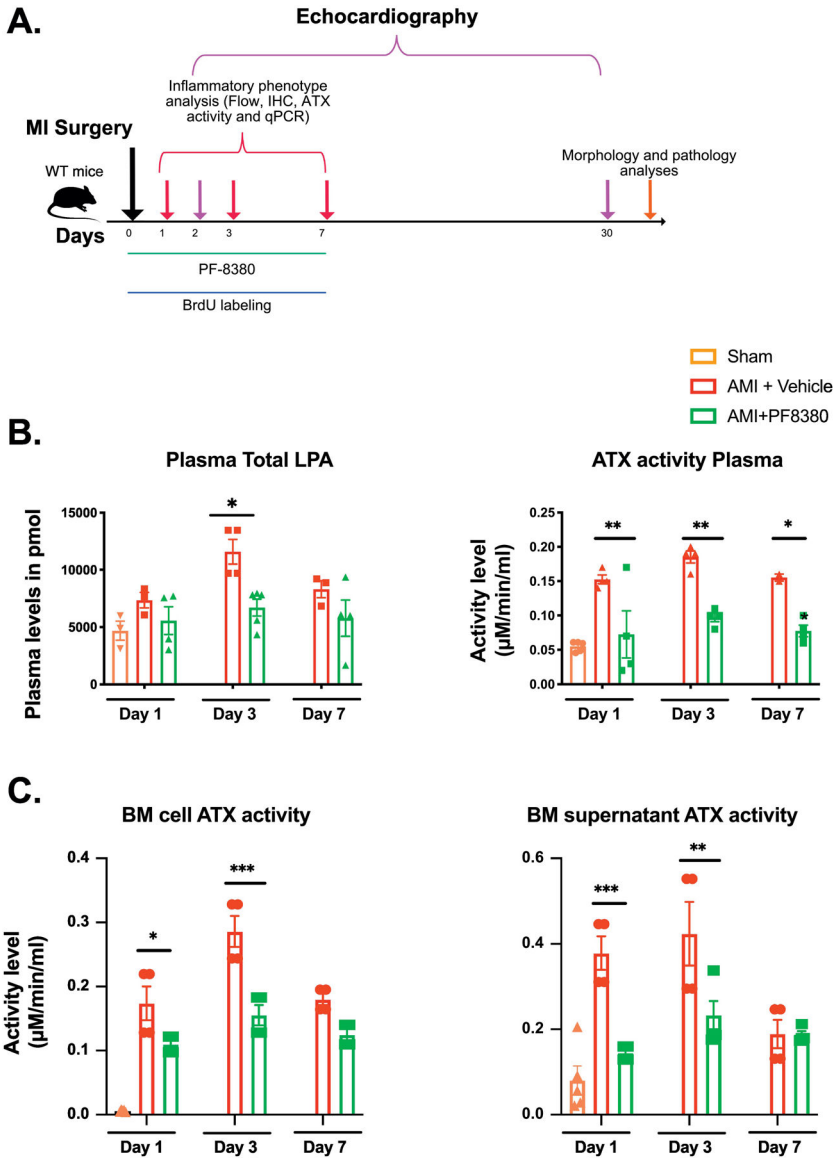

Figure 6. Autotaxin inhibitor PF8380 attenuates plasma LPA and ATX activity in wild type mice.

Female C57BL/6 mice, aged 8–10 weeks were randomized to receive PF8380 at 10 mg/kg i.p. twice daily or vehicle for 7 days after LAD ligation. **(A)** Experimental design for the *in vivo* study **(B)** Post LAD ligation on day 1,3 and 7 plasma total LPA levels and ATX activity were measured by mass spectrometry and choline release assay, respectively. Plasma LPA level and ATX activity were elevated after AMI. Mice treated with PF8380 showed significant reduction in plasma LPA level and ATX activity during the peak inflammatory response. **(C)** ATX activity in bone marrow cells and supernatant post AMI showed significant increase in days 1 and 3. This effect was blunted when mice were treated with ATX inhibitor PF8380 (n=4–6 mice/group/time-point). Comparison between groups was performed by repeated measures ANOVA, *$P \leq 0.05$, **$P \leq 0.01$, ***$P \leq 0.001$. ATX, autotaxin; BrdU, Bromodeoxyuridine/5-bromo-2'-deoxyuridine; LPA, lysophosphatidic acid.

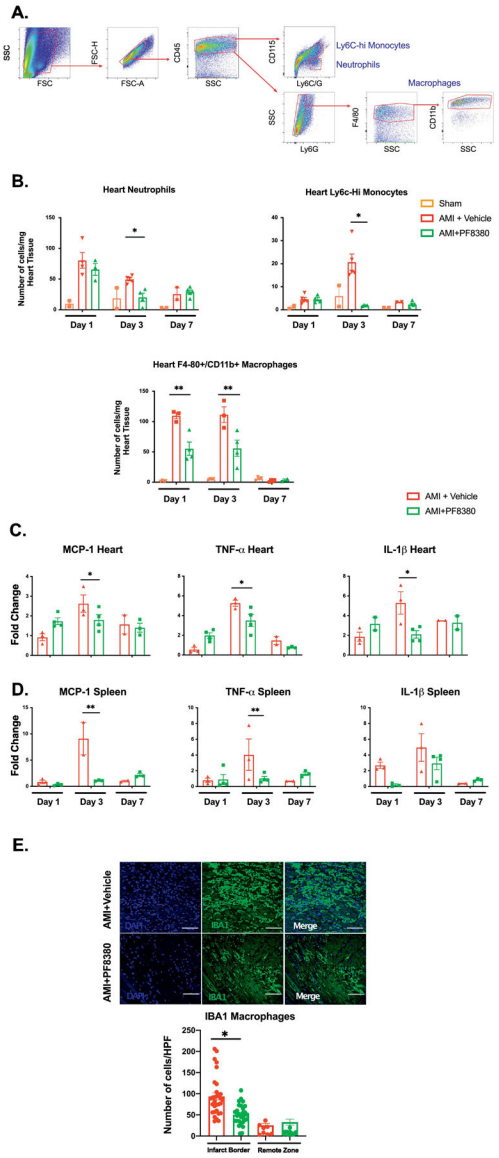

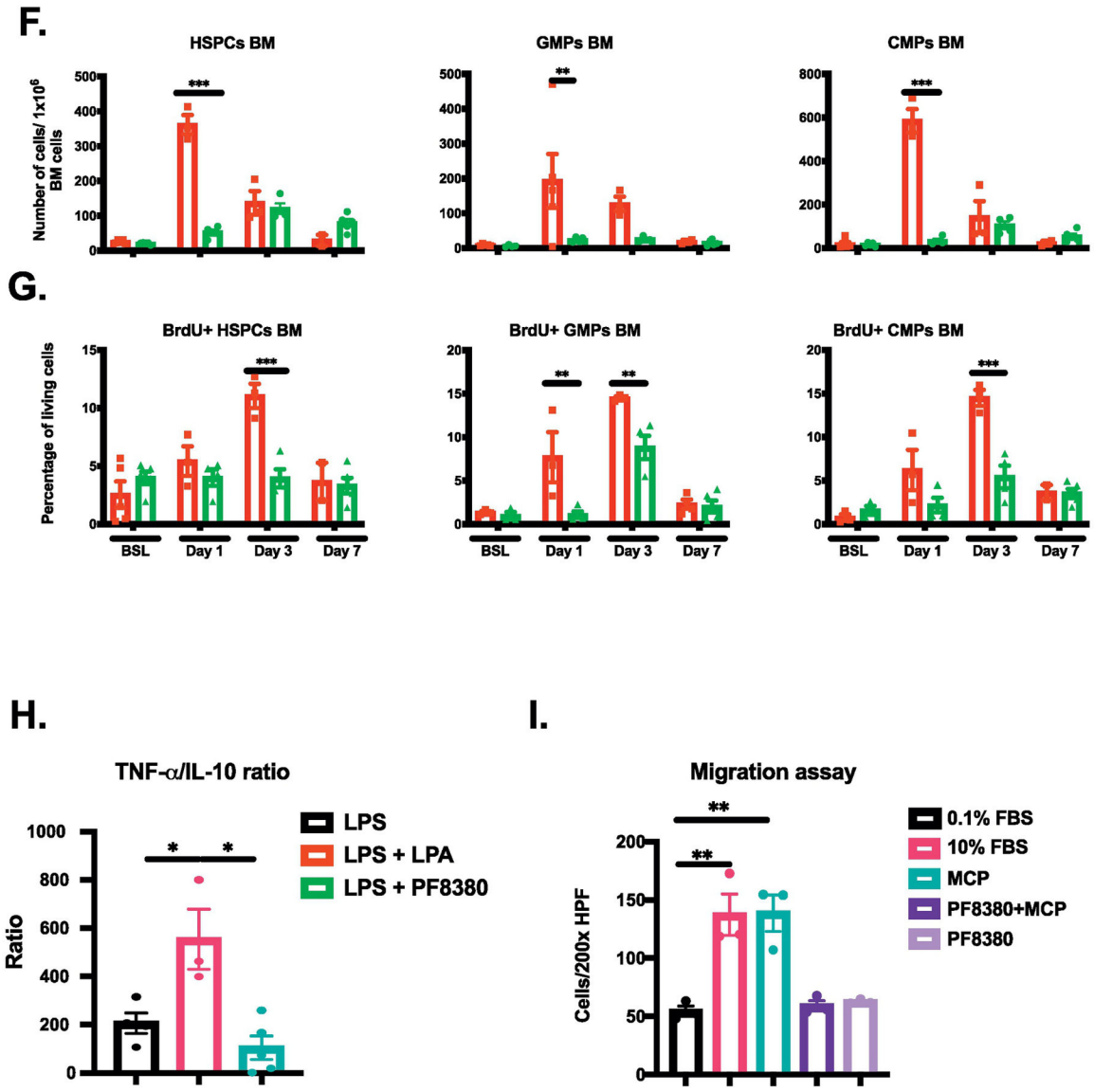

Figure 7: Autotaxin inhibitor PF8380 reduces number of cardiac inflammatory cells, number and proliferation of bone marrow derived myeloid progenitor cells and pro- inflammatory cytokines in *in vivo* and bone marrow derived macrophages.

(A) Representative FACS plots demonstrating gating strategy for inflammatory cells. **(B)** Cardiac neutrophil numbers ($CD45^{+}/CD115^{lo}/Ly6C/G^{hi}$), $Ly6C^{hi}$ monocytes ($CD45^{+}/Ly6C/G^{hi}/CD115^{hi}$), and the pro-inflammatory macrophages ($F4\text{-}80^{+}$) and ($CD45^{+}/F4\text{-}80^{+}/CD11b^{+}$) were reduced in PF8380 treated mice at day 3 compared to vehicle controls. **(C and D)** Gene expression of pro-inflammatory cytokines IL-1β, MCP-1 and TNF-α in heart and spleen were significantly reduced in mice treated with autotaxin inhibitor compared to vehicle controls. (N=4–6 mice/group/time-point, bone marrow derived macrophages data is representative of 5 independent experiments. **(E)** Representative image of Immunohistochemical staining for macrophage marker IBA1 (green) in the heart section post MI on day 3. Quantitative analysis of IBA1 in infract border and remote zone showed decrease number in autotaxin inhibitor treated mice Scale bars represent 50 μm **(F and G)**

Flow cytometry analyses of absolute hematopoietic progenitor number and percentage of $BrdU^+$ cells showing a significant reduction in number and proliferation of HSPCs (Sca1+/c-Kit+/Lin-), GMPs (Lin-/c-Kit+/Sca-1-/CD16/32+/CD34+) and CMPs (Lin-/c-Kit+/Sca-1+CD16/32-/CD34+) in bone marrow of WT mice treated with PF8380 compared to vehicle controls (n=4 mice/group/time-point). **(H)** Quantitative analyses of pro-inflammatory macrophage-conditioned media using ELISA reveals that the ratio of proinflammatory cytokine, TNF-α, and the anti-inflammatory cytokine, IL-10 ratio was high in presence of LPA but significantly reduced in the presence of the specific autotaxin inhibitor, PF8380. **(I)** Quantification of bone marrow derived macrophage migration using Transwell migration assay showing reduction in macrophage migration after ATX inhibition. BMDM migrated readily towards MCP-1 (20 ng/ml) but this migration was blunted after 2-hour pre-incubation with PF8380 (10μM). Comparison between groups was performed by repeated measures ANOVA [Panel B, C,D,F and G] or one-way ANOVA [Panel H and I]; $*P \leq 0.05$, $**P \leq 0.01$,$***P \leq 0.001$. ATX, autotaxin; AMI, Acute Myocardial Infarction; BrdU, Bromodeoxyuridine/5-bromo-2'-deoxyuridine; BM, bone marrow; CMPs: Common myeloid progenitors; GMPs, Granulocyte macrophage progenitors; HSPCS; Hematopoietic stem progenitor cells HPF; high power field; IL-1β, Interleukin 1 beta; IL-10, interleukin 10; LPA, lysophosphatidic acid; MCP-1, Monocyte chemoattractant protein-1; TNF-α, tumor necrosis factor alpha.

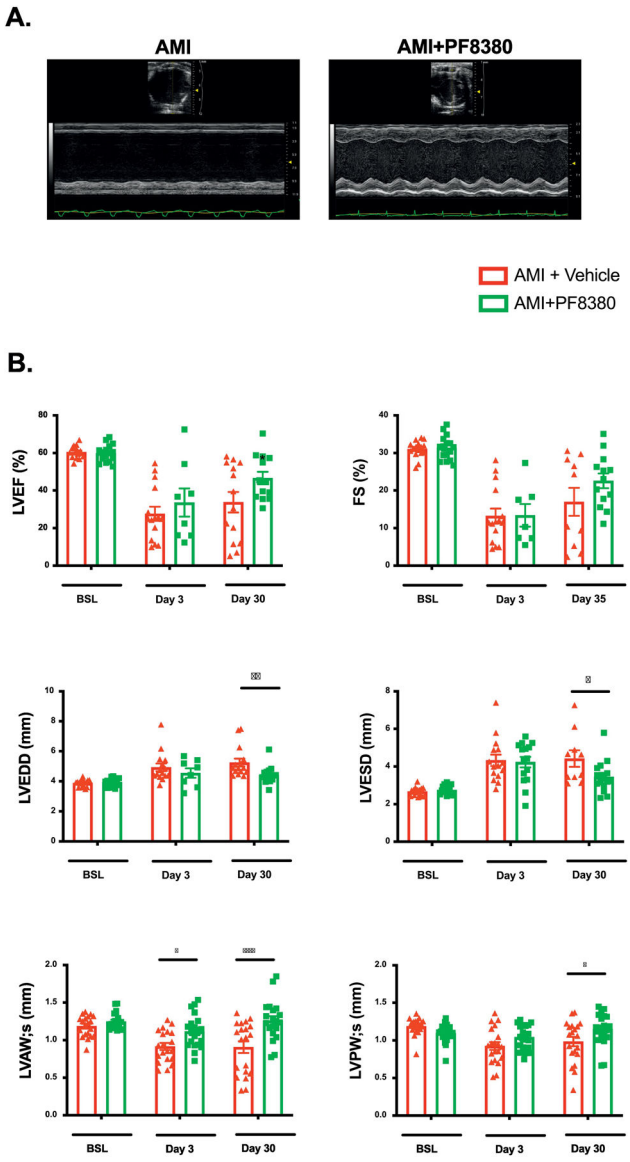

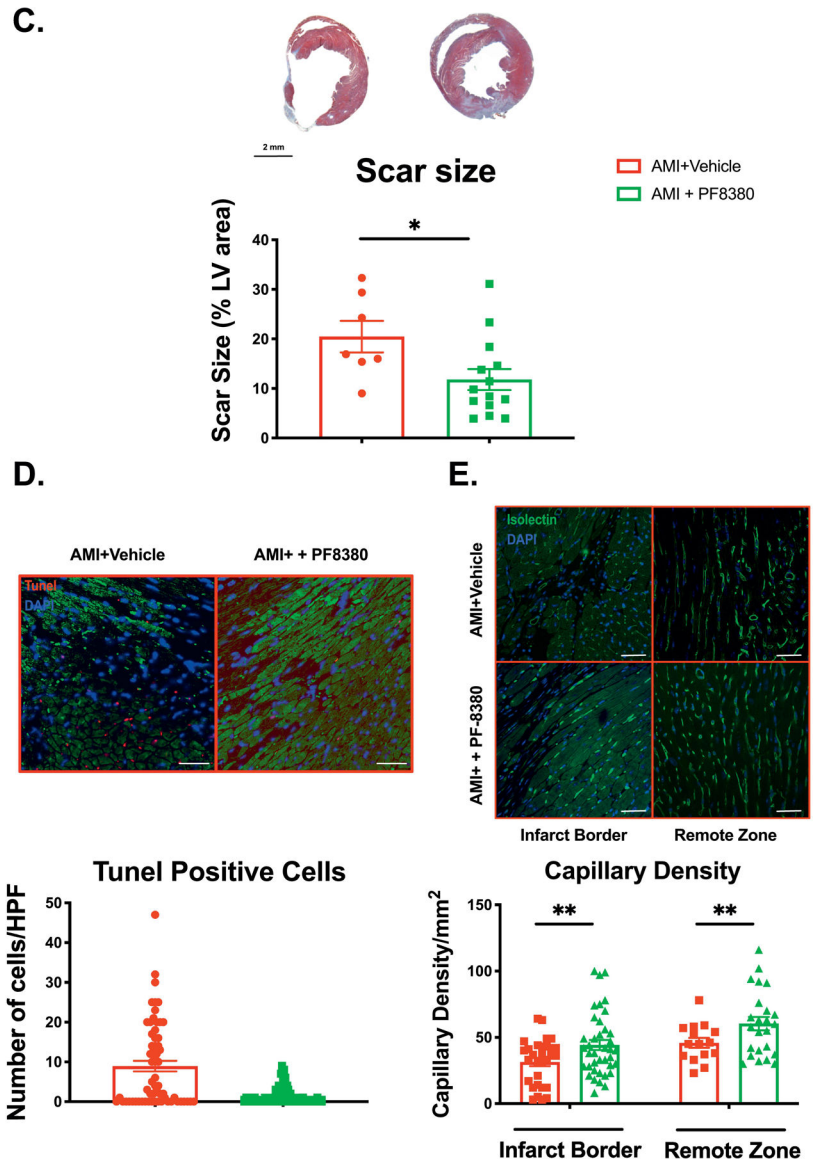

Figure 8: Autotaxin inhibition improves cardiac functional recovery, scar size, reduces apoptosis and adverse remodeling post-AMI.

(A) 30 days following AMI, transthoracic echocardiography using M-Mode and 2D echocardiography was performed on control and ATX inhibitor treated mice to evaluate left ventricular function and remodeling parameters. **(B)** Cardiac function improved after myocardial infarction in ATX inhibitor treated mice compared to vehicle controls. Quantitative analyses demonstrate significant improvement in LV function as assessed by LVEF and fractional shortening. Data also shows significant improvement in left ventricular adverse remodeling parameters such as left ventricular end-systolic and end-diastolic diameter. **(C)** Representative picture shows Masson's trichrome staining done at 30 days after LAD ligation. Quantitative analysis of scar as percentage of LV area showed significant reduction in scar size of inhibitor group mice. **(D)** Representative TUNEL positive (red) image for apoptotic cells in the peri-infarct region of cardiomyocytes stained by α-sarcomeric actin (green) in control and ATX inhibitor treated mice demonstrates more

TUNEL positive cells in control group mice. Quantitative analysis of TUNEL positive cells confirms less apoptosis in PF8380 group mice (n=8–10 mice/group/time-point), **(E)** Representative isolectin staining (green) image for capillary density in the peri-infarct region in control and ATX inhibitor treated mice demonstrates high capillary density in PF8380 group mice. Quantitative analysis of capillary density confirms higher angiogenesis and capillary density in PF8380 group mice (n=8–10 mice/group/time-point, n=3–4 mice/group/time-point, for TUNEL staining). Comparison between groups was performed by repeated measures ANOVA [Panel B] or Student *t*-test [Panels C, D and E], *$P \leq 0.05$, **$P \leq 0.01$ AMI, Acute Myocardial Infarction; ATX, autotaxin; FS, fractional shortening; LAD, left anterior descending artery; LV, left ventricular; LVAWs, left ventricular anterior wall thickness in systole; LVEF, left ventricular ejection fraction; LVEDD, left ventricular end-diastolic diameter; LVESD, left ventricular end-systolic diameter; LVPWs, left ventricular posterior wall thickness in systole. Scale bars for panels D and E 50 μm

Table 1.

Clinical characteristics of patients included in the study.

Demographic and clinical parameters	N (%) or mean (SD)	
	Control	STEMI patients
Age	51 (21)	59.1 (11.7)
Female	2 (40)	12 (21)
Body mass index (BMI)	26.4 (4.3)	29.0 (5.6)
Left ventricular ejection fraction	N/A	47.7 (8.6)
Plasma troponin	N/A	3.4 (3.7)
Diabetes	3 (60)	12 (30)
Hypertension	3 (60)	28 (70)
Hyperlipidemia	2 (40)	11 (27.5)
Congestive heart failure	2 (40)	0 (0)
Current smokers	1 (20)	20 (50)
Race		
White	5 (100)	37 (92.5)
African American	0 (0)	2 (5)
Culprit artery	N/A	
Left anterior descending		12 (30)
Left circumflex		6 (15)
Right coronary artery		21 (52.5)
Previous myocardial infarction	1 (20)	4 (10)
Previous coronary revascularization	1 (20)	12 (30)
Previous coronary bypass surgery	1 (20)	0 (0)
Previous stroke	0 (0)	1 (2.5)
Peripheral vascular disease	0 (0)	1 (2.5)
Chronic kidney disease	0 (0)	0 (0)
Medications		
Statins	4 (80)	10 (25)
Angiotensin converting enzyme	0 (0)	8 (20)
Angiotensin receptor blocker	1 (20)	3 (7.5)
Beta Blocker	1 (20)	13 (32.5)
Aspirin	4 (80)	14 (35)

Table 2.

Correlation between plamsa LPA level and circulating inflammatory cells.

Cell population	Pearson correrlation coofecient	P value
Granulocytes	0.546	<0.01
CD11b+ granultocytes	0.862	<0.01
CCR2+ granulocytes	0.532	<0.01
Total monocytes	0.704	<0.01
CD11b+/CD14+/CD16- monocytes	0.538	<0.01
CD11b+/CD14-/CD16+ monocytes	0.928	<0.01
CD42b+/CD14-/CD16+ monocytes	0.809	<0.01
CCR2+/CD14-/CD16+ monocytes	0.643	<0.01

CCR2+ granulocytes indicate monocyte-granulocyte aggregates.

Table 3.

Echocardiographic parameters.

LPP3 study				
	Mx1-Plpp3$^{fl/fl}$		**Mx1-Plpp3$^{\Delta}$**	
	BSL	**1 month**	**BSL**	**1 month**
Heart rate	442.6 ± 5.8	462.5 ± 9.2	431.2 ± 24.7	465.1 ± 35.7
Stroke volume	35.4 ± 1.4	27.3 ± 3.6	38.3 ± 1.6	39.9 ± 5.7*
Cardiac output	15.7 ± 0.7	12.5 ± 1.6	16.4 ± 0.8	18.96 ± 3.1*
Anterior wall thickness (diastole)	1.76 ± 0.03	0.723 ± 0.06	0.7 ± 0.02	0.77 ± 0.02
Posterior wall thickness (diastole)	0.82 ± 0.04	0.72 ± 0.05	0.76 ± 0.03	0.77 ± 0.03
Autotaxin inhibition study				
	Vehicle		**PF-8380**	
	BSL	**1 month**	**BSL**	**1 month**
Heart rate	438 ± 7.3	477 ± 9.6	441 ± 6.5	479 ± 8.7
Stroke volume	39.7 ± 0.85	24.4 ± 4.48	39.1 ± 0.8	35.4 ± 2.2*
Cardiac output	**17.4** ± 0.5	14.4 ± 1.7	17.1 ± 0.6	17.6 ± 0.7*
Anterior wall thickness (diastole)	0.78 ± 0.02	0.62 ± 0.05	0.79 ± 0.02	0.8 ± 0.03*
Posterior wall thickness (diastole)	0.85 ± 0.02	0.87 ± 0.02	0.78 ± 0.02	0.82 ± 0.05

Data presented as mean ± standard error of means.

*P <0.05 (2 way ANOVA with Sidak correction method for multiple comparisons).